

# Synchronization in $\mathcal{PT}$ -symmetric optomechanical resonators

Chang-long Zhu,<sup>1</sup> Yu-long Liu,<sup>2</sup> Lan Yang,<sup>3</sup> Yu-xi Liu,<sup>2,4,\*</sup> and Jing Zhang<sup>1,4,†</sup>

<sup>1</sup>*Department of Automation, Tsinghua University, Beijing 100084, P. R. China*

<sup>2</sup>*Institute of Microelectronics, Tsinghua University, Beijing 100084, P. R. China*

<sup>3</sup>*Department of Electrical and Systems Engineering,  
Washington University, St. Louis, MO 63130, USA*

<sup>4</sup>*Center for Quantum Information Science and Technology, BNRist, Beijing 100084, P. R. China*

(Dated: April 7, 2020)

Synchronization has great impacts in various fields such as self-clocking, communication, neural networks, etc. Here we present a mechanism of synchronization for two mechanical modes in two coupled optomechanical resonators via optical coupling of the cavity fields by introducing the so-called  $\mathcal{PT}$ -symmetric structure. It is shown that the degree of synchronization between the two far-off-resonant mechanical modes can be increased by decreasing the coupling strength between the two optomechanical resonators. Furthermore, when we consider the stochastic noises in the optomechanical resonators, we find that more noises can enhance the degree of synchronization of the system under particular  $\mathcal{PT}$ -symmetric condition. Our results reveal versatile effects of optical  $\mathcal{PT}$ -symmetry on controlling the synchronization dynamics of indirect coupled mechanical resonators. parameter regime.

PACS numbers: 05.45.Xt,07.10.Cm,45.50.Wk,42.65.-k

## I. INTRODUCTION

Synchronization is a phenomenon in which two or more systems coordinate and act at the same time with similar behavior. Synchronization determined phenomenon such as the chorusing of crickets, a flash of fireflies, pendulum clocks, and even the life cycle of creatures [1–3] have been extensively observed in our daily life. In particular, synchronization, the rhythms of two or more different objects adjusted in unison, is a qualitative transition and thus motivates wide applications in various fields, such as data communication, timekeeping, navigation, cryptography, and neuroscience [4–9].

Benefiting from current advanced nano-fabrication techniques, especially those for high-quality-factor on-chip optomechanical resonators [10], it is possible to demonstrate the synchronization of resonators in on-chip nano-scale platforms [11–16]. For example, a pair of closely placed optomechanical resonators with different mechanical frequencies were synchronized by indirect coupling through the coupled optical fields [13]. More recently, two nanomechanical oscillators separated for about 80  $\mu\text{m}$  were synchronized through the same optical field in an optical racetrack [14].

In this paper, we show that mechanical oscillations can be synchronized by optomechanical couplings to two coupled optical modes, in which one is active and the other one is passive. With balanced gain and loss, such kinds of systems are called parity-time ( $\mathcal{PT}$ )-symmetric optomechanical systems, which have attracted great attentions in recent years [17–23]. Various appealing phenomena

and important applications have been proposed in particular systems with  $\mathcal{PT}$ -symmetric structure [17–44].

Although the optomechanical interaction has influence on our  $\mathcal{PT}$ -symmetric system, this influence is negligibly small under the parameter regime we consider [18–22]. By introducing the  $\mathcal{PT}$ -symmetric structure, we observe an interesting phenomenon that the two mechanical modes of the coupled optomechanical resonators tend to oscillate in unison by decreasing the optical coupling strength between them. This observation somewhat conflicts with the normal phenomenon that: the stronger coupling strength between two systems is, the easier the synchronization can be realized. Another counterintuitive phenomenon presented as the enhancement of synchronization between the two mechanical modes when considering the noises acting on the optomechanical resonators.

## II. COUPLED-OPTOMECHANICAL RESONATORS WITH OPTICAL $\mathcal{PT}$ -SYMMETRY

The system we consider consists of two coupled whispering-gallery-mode (WGM) resonators, and is depicted in Fig. 1(a). The left WGM resonator ( $\mu C_1$ ) is an active one which can be realized, e.g., by  $\text{Er}^{3+}$ -doped silica disk, and the right one ( $\mu C_2$ ) is a passive resonator. Each resonator supports an optical mode  $\alpha_i$  and a mechanical mode  $\beta_i$  ( $i = 1, 2$ ), and the inter-cavity optical coupling strength  $\kappa$  between  $\alpha_1$  and  $\alpha_2$  is related to the distance between the two resonators. As is well known, although the two mechanical modes  $\beta_1$  and  $\beta_2$ , located in two different resonators, are not directly coupled, they can be indirectly coupled through the inter-cavity optical coupling and the intra-cavity optomechanical coupling. We elaborate this indirect mechanical coupling in

\*Electronic address: yuxiliu@mail.tsinghua.edu.cn

†Electronic address: jing-zhang@mail.tsinghua.edu.cn

Fig. 1(b). Each WGM resonator is equivalent to a Fabry-Perot cavity, with one fixed mirror and one movable one. The optical modes  $\alpha_1$  and  $\alpha_2$  represent the optical fields in the Fabry-Perot cavities and the mechanical modes  $\beta_1$  and  $\beta_2$  indicate the motions of the movable mirrors. In each equivalent Fabry-Perot cavity, the movable mirror suffers a radiation-pressure force induced by the optical mode  $\alpha_i$  ( $i=1,2$ ). Such a force is proportional to the circulating optical intensity  $|\alpha_i|^2$  in the cavity, which leads to the mechanical motion  $\beta_i$ . In the meantime, the movable mirror induces a frequency-shift of the optical mode in the cavity, which influences the dynamics of  $\alpha_i$ . In Fig. 1(b),  $\alpha_1$  ( $\alpha_2$ ) and  $\beta_1$  ( $\beta_2$ ) interact with each other through this kind of radiation-pressure coupling, and  $\alpha_1$  and  $\alpha_2$  are directly coupled through the inter-cavity evanescent optical fields. Therefore, the mechanical modes  $\beta_1$  and  $\beta_2$  are coupled indirectly by the evanescent optical coupling between  $\alpha_1$  and  $\alpha_2$ .

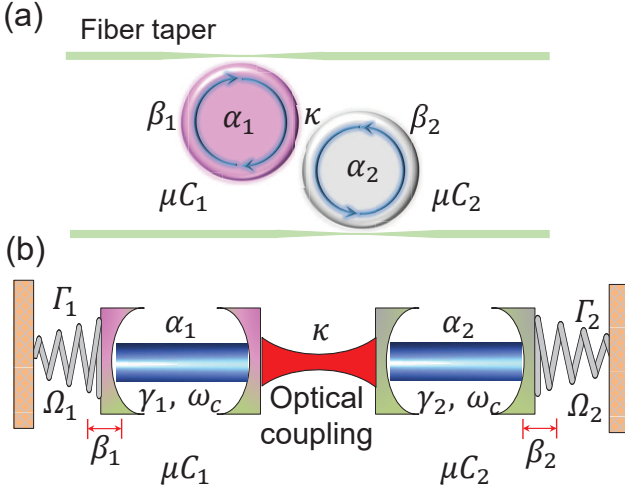


FIG. 1: (color online) Schematic diagram of the optically-coupled  $\mathcal{PT}$  optomechanical system. (a)  $\mu C_1$  denotes an active WGM resonator with gain medium and  $\mu C_2$  is a passive one. (b) Equivalent diagram of the  $\mathcal{PT}$  optomechanical system, where the WGM resonators are replaced by Fabry-Perot cavities with a moveable end mirror and a fixed one. The two cavities are directly coupled through the inter-cavity evanescent optical fields, and the optical coupling strength  $\kappa$  depends on the distance between the two Fabry-Perot cavities [13].

The  $\mathcal{PT}$ -optomechanical system we consider can be represented by the following equations:

$$\begin{aligned} \dot{\alpha}_1 &= -\Gamma_{\text{op}1}\alpha_1 - i\kappa\alpha_2 - ig_{\text{om}}\alpha_1(\beta_1 + \beta_1^*) + \sqrt{2\gamma_{1\text{ex}}}\epsilon_1, \\ \dot{\alpha}_2 &= -\Gamma_{\text{op}2}\alpha_2 - i\kappa\alpha_1 - ig_{\text{om}}\alpha_2(\beta_2 + \beta_2^*) + \sqrt{2\gamma_{2\text{ex}}}\epsilon_2, \\ \dot{\beta}_1 &= -(\Gamma_{m1} + i\Omega_1)\beta_1 - ig_{\text{om}}|\alpha_1|^2, \\ \dot{\beta}_2 &= -(\Gamma_{m2} + i\Omega_2)\beta_2 - ig_{\text{om}}|\alpha_2|^2, \end{aligned} \quad (1)$$

where  $\Gamma_{\text{op}1} = -\gamma_1 + i\Delta_1$  and  $\Gamma_{\text{op}2} = \gamma_2 + i\Delta_2$ .  $\gamma_i$ ,  $\gamma_{\text{ex}}$ ,  $\Delta_i = \omega_{ci} - \omega_L$ , and  $\epsilon_i$  ( $i = 1, 2$ ) denote the gain (loss) rate of the resonator  $\mu C_i$ , the external damping rate in-

duced by the coupling between the resonator and the input/output fiber-taper, the detuning frequency between the resonance frequency ( $\omega_{ci}$ ) of the cavity mode and the frequency ( $\omega_L$ ) of the driving field, and the amplitude of the driving field, respectively. Without loss of generality, here we assume that  $\Omega_2 \geq \Omega_1$ .  $\Omega_i$  and  $\Gamma_{mi}$  represent the frequency and damping rate of the mechanical mode  $\beta_i$ . To simplify our discussion, we assume that the gain cavity  $\mu C_1$  and the lossy cavity  $\mu C_2$  have the same vacuum optomechanical coupling strength  $g_{\text{om}}$  which quantifies the interaction between a single photon and a single phonon. We also assume that the gain rate of  $\mu C_1$  is equal to the damping rate of  $\mu C_2$ , i.e.,  $\gamma_2 = \gamma_1 \equiv \gamma$ , which means that the gain and loss in the system are well balanced. Additionally, we consider the case of critical coupling such that  $\gamma_{1\text{ex}} = \gamma_{2\text{ex}} = \gamma/2$ .

In general, the vacuum optomechanical coupling strength  $g_{\text{om}}$  of typical optical cavities is very small [10], and thus that the influence of optomechanical interaction on optical structure in our system can be ignored. Under the condition of symmetric optical driving detunings ( $\Delta_- = \Delta_2 - \Delta_1 = 0$ ), there exists a phase transition point, called exceptional point (EP) [18–22], corresponding to a critical inter-cavity coupling strength  $\kappa_{\text{EP}} = \gamma$ . When  $\kappa > \kappa_{\text{EP}}$  which is in so-called  $\mathcal{PT}$ -symmetric regime, there exist two non-degenerate optical supermodes with the same damping rate. When  $\kappa \leq \kappa_{\text{EP}}$  which is in the so-called broken  $\mathcal{PT}$ -symmetric regime, the two optical supermodes are degenerate but with different damping rates. When the system is far away from the EP, the interaction between the optical supermodes and mechanical modes, i.e. the effective radiation-pressure coupling in the supermode picture, is weak. This kind of interaction will be greatly enhanced as  $\kappa$  approaches to  $\kappa_{\text{EP}}$ . This results from the topological-singularity-induced amplification of the optomechanical nonlinearity in the vicinity of the exceptional point [18–21, 23].

However, slightly different from Refs [18–22], in this work we consider asymmetric optical driving detunings, i.e.,  $\Delta_- = \Delta_2 - \Delta_1 \neq 0$ , in order to synchronize the two mechanical modes which will be discussed in the following section. The difference between the two optical driving detunings  $\Delta_-$  is small enough that the properties of  $\mathcal{PT}$ -symmetric structure in our system is still held, i.e., the optomechanical interaction can still be greatly amplified near the exceptional point. Here, we consider the condition (see Appendix A)

$$g_{\text{om}} \ll \Delta_- \ll \sqrt[3]{\frac{2}{3}\gamma \left( g_{\text{om}}^2 \frac{\Omega_2 + \Omega_1}{\Omega_1 \Omega_2} \gamma \epsilon^2 \right)^2} \ll \gamma, \kappa, \quad (2)$$

then the non-degeneracy between the optical supermodes at exceptional point can be approximated given by

$$\frac{\Delta_{\text{split}}}{\gamma} \approx \sqrt{\frac{\Delta_-^3}{\frac{2}{3}\gamma \left( g_{\text{om}}^2 \frac{\Omega_2 + \Omega_1}{\Omega_1 \Omega_2} \gamma \epsilon^2 \right)^{2/3}}},$$

where  $\Delta_{\text{split}} = \text{Im}[\omega_{o+} - \omega_{o-}] = \text{Re}[\omega_{o+} - \omega_{o-}]$ , and  $\omega_{o\pm}$  are the eigenvalues of optical supermodes. It is clear that this non-degeneracy  $\Delta_{\text{split}}$  is very small that the  $\mathcal{PT}$ -symmetric structure in our system is still held.

Given the system parameters  $\gamma = 30$  MHz,  $\Delta_1 = 4.2$  MHz,  $\Delta_2 = 5$  MHz,  $\Omega_1 = 5$  MHz,  $\Omega_2 = 15$  MHz,  $\Gamma_{m1} = 8$  kHz,  $\Gamma_{m2} = 8$  kHz,  $g_{om} = 3$  kHz, and  $\epsilon = 70$  MHz $^{1/2}$ , the simulation results of the mode splitting and linewidth of the optical supermodes are shown in Figs. 2 (a) and (b). It is obvious that the non-

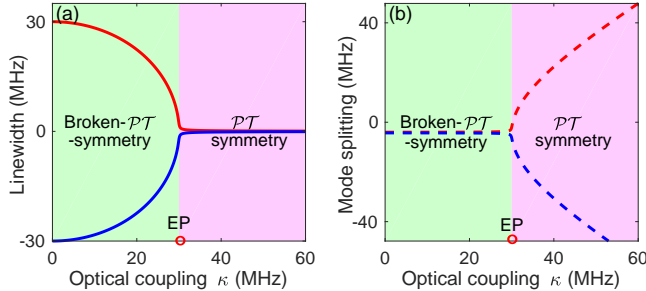


FIG. 2: (Color online) (a) Linewidth of the supermodes, i.e., the real parts of the eigenfrequencies, (b) mode splitting of the supermodes, i.e., the imaginary parts of the eigenfrequencies. The green region is the broken- $\mathcal{PT}$ -symmetry regime, the pink region corresponds to the  $\mathcal{PT}$ -symmetric regime.

degeneracy at EP in Fig. 2 is negligibly small, and the broken- $\mathcal{PT}$ -symmetric and  $\mathcal{PT}$ -symmetric regimes can be clearly observed. It should be noted that although one eigenfrequency of the optical supermodes has the positive real component in the broken- $\mathcal{PT}$ -symmetric regime (Fig. 2(a)), the saturation nonlinearity induced by the optomechanical coupling will suppress the divergence induced by this positive rate [45, 46].

### III. FREQUENCY SYNCHRONIZATION VIA $\mathcal{PT}$ -SYMMETRY

When the degrees of freedom of the optical modes are adiabatically eliminated under the condition that the optical decay rates are much larger than the mechanical decay rates, the enhanced optomechanical coupling, induced by the topological-singularity-induced amplification of the optomechanical nonlinearity, will lead to significant effective frequency shifts  $\delta\Omega_1$  and  $\delta\Omega_2$  for the mechanical modes  $\beta_1$  and  $\beta_2$  in the vicinity of EP. In fact, under the condition depicted in Eq. (2) and  $\epsilon_1 = \epsilon_2 \equiv \epsilon$ ,  $\delta\Omega_1$  and  $\delta\Omega_2$  near EP can be written as (detailed derivation see Appendix C)

$$\delta\Omega_1 = -\delta\Omega_2 \approx \frac{g_{om}^2 \Delta_- (\gamma^2 + \kappa^2)^2 \gamma \epsilon^2}{[(\kappa^2 - \gamma^2)^2 + \gamma^2 \Delta_-^2]}. \quad (3)$$

Here, in order to synchronize the two mechanical oscillators, we require that  $\Delta_1$  and  $\Delta_2$  have small difference, which makes sure that  $\delta\Omega_1$  and  $\delta\Omega_2$  are opposite in sign,

and the influence on the structure of  $\mathcal{PT}$ -symmetry is very small simultaneously.

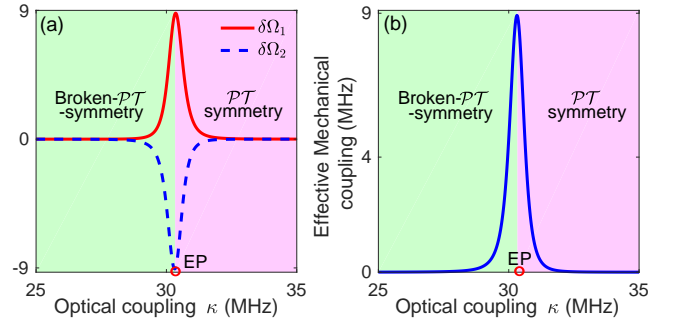


FIG. 3: (Color online) (a) Optomechanics-induced mechanical frequency shifts  $\delta\Omega_{1,2}$  of the two optomechanical resonators versus the optical coupling strength  $\kappa$  both in broken- $\mathcal{PT}$ -symmetric regime and  $\mathcal{PT}$ -symmetric regime. (b) Effective coupling strength  $\kappa_{\text{mech}}$  between two mechanical modes versus the optical coupling strength  $\kappa$ .

We show in Fig. 3(a) the optomechanics-induced mechanical frequency shift  $\delta\Omega_i$  (red-solid curve) and  $\delta\Omega_2$  (blue-dashed curve) of the two resonators versus the optical coupling strength  $\kappa$ , both in broken- $\mathcal{PT}$ -symmetric and  $\mathcal{PT}$ -symmetric regimes. When the system is far away from the exceptional point, the optomechanics-induced mechanical frequency shift  $\delta\Omega_i$  is negligibly small. However,  $\delta\Omega_i$  will be greatly enhanced such that  $\delta\Omega_i$  is almost comparable with or even larger than  $\Omega_i$ , when  $\kappa$  approaches to  $\kappa_{\text{EP}}$ . As these two enhanced frequency shifts for the mechanical modes are opposite in sign, they will lead to significant modifications of mechanical frequencies  $\Omega_1$  and  $\Omega_2$ , and make the two mechanical frequencies  $\Omega_1$  and  $\Omega_2$  to approach each other. Thus the two oscillators tend to be resonant with each other, and occurs synchronization.

Moreover, the enhanced optomechanical coupling can also induce an enhancement of the effective mechanical interaction between mechanical modes  $\beta_1$  and  $\beta_2$  in the vicinity of the EP. In fact, by adiabatically eliminating the degrees of freedom of the optical modes, we obtain the effective coupling strength  $\kappa_{\text{mech}}$  between the two mechanical modes  $\beta_1$  and  $\beta_2$  as

$$\kappa_{\text{mech}} \approx \frac{4g_{om}^2 \Delta_- \kappa^2 \gamma^3 \epsilon^2}{[(\kappa^2 - \gamma^2)^2 + \gamma^2 \Delta_-^2]}. \quad (4)$$

In Fig. 3(b) the effective mechanical coupling strength  $\kappa_{\text{mech}}$  versus the optical coupling strength  $\kappa$  is plotted, both in broken- $\mathcal{PT}$ -symmetric and  $\mathcal{PT}$ -symmetric regimes. It can be clearly seen that the effective mechanical coupling strength  $\kappa_{\text{mech}}$  is negligibly small when the system is far away from the exceptional point, but can be significantly enhanced when  $\kappa$  approaches to  $\kappa_{\text{EP}}$ . This enhanced effective mechanical interaction in the vicinity of the EP can also contribute to synchronization between the two mechanical modes  $\beta_1$  and  $\beta_2$ , since the enhanced

$\kappa_{\text{mech}}$  can greatly change the mechanical frequencies  $\Omega_1$  and  $\Omega_2$  and make the two mechanical frequencies to get close to each other (detailed discussion can be found in Appendix D).

Actually, the effective mechanical frequencies of the two mechanical oscillators in the vicinity of the EP can be expressed as  $\Omega_{1,\text{eff}} = \Omega_1 + \delta\Omega_1 + \delta\Omega_{\text{coup}}$  and  $\Omega_{2,\text{eff}} = \Omega_2 + \delta\Omega_2 - \delta\Omega_{\text{coup}}$ , respectively, where  $\delta\Omega_{\text{coup}}$  is induced by the effective mechanical coupling strength  $\kappa_{\text{mech}}$  (see Appendix D). This means that the enhanced optomechanics-induced mechanical frequency shifts  $\delta\Omega_1/\delta\Omega_2$  and effective mechanical coupling strength  $\kappa_{\text{mech}}$  can result in significant modifications of mechanical frequencies  $\Omega_1/\Omega_2$  together, and thus jointly contribute to the synchronization between the two mechanical oscillators, i.e.,  $\Omega_{1,\text{eff}} = \Omega_{2,\text{eff}}$ . We show in Fig. 4(a) that the effective mechanical frequencies  $\Omega_{1,\text{eff}}$  (red-solid curve) and  $\Omega_{2,\text{eff}}$  (blue-dashed curve) of the two resonators versus the optical coupling strength  $\kappa$ , both in broken- $\mathcal{PT}$ -symmetric and  $\mathcal{PT}$ -symmetric regimes. It is clear that the two mechanical oscillators tend to be resonant with each other, i.e.,  $\Omega_{1,\text{eff}} = \Omega_{2,\text{eff}}$ , and thus synchronize, when  $\kappa$  approaches to  $\kappa_{\text{EP}}$ . As is well known, the frequency-mismatch between two synchronized oscillators should be very small in traditional lossy systems [12, 13], i.e.,  $|\Omega_1 - \Omega_2| \ll \Omega_1, \Omega_2$ . However, as shown in Fig. 4, our  $\mathcal{PT}$ -symmetric system can perfectly synchronize two far-off-resonant mechanical oscillators. Actually, as shown in Fig. 4(a), the effective mechanical frequencies of the two optomechanical resonators  $\Omega_{1,\text{eff}}$  and  $\Omega_{2,\text{eff}}$  coincide with each other when  $\kappa$  approaches  $\kappa_{\text{EP}}$ .

In addition, we find an counterintuitive phenomenon that *weaker* coupling between two optomechanical resonators may be *helpful* for synchronization for our  $\mathcal{PT}$  optomechanical system. In fact, as shown in Fig. 4(a), in the  $\mathcal{PT}$ -symmetric regime (the pink region), when the coupling strength  $\kappa$  between two resonators is *decreased*, the effective mechanical frequencies of the two resonators tend to coincide with each other, which means that  $\beta_1$  and  $\beta_2$  are inclined to oscillate in unison with the weaker coupling strength  $\kappa$  in the  $\mathcal{PT}$ -symmetric regime. The broken- $\mathcal{PT}$ -symmetric regime is the normal regime where stronger coupling between the two optomechanical resonators makes the two mechanical modes  $\beta_1$  and  $\beta_2$  be inclined to be synchronized. We can more easily see this phenomenon by plotting the spectra of the normalized mechanical displacements of the two optomechanical resonators  $x_1 = (\beta_1 + \beta_1^*)/2$  (the red solid curve) and  $x_2 = (\beta_2 + \beta_2^*)/2$  (the blue dashed curve) in Figs. 4(c) and (d), where  $\kappa$  is increased from 2 MHz to 29.86 MHz in Fig. 4(c), and is decreased from 50 MHz to 30.81 MHz in Fig. 4(d).

To give more insights into the phenomena shown by us, we plot in Fig. 4(b) the cross-correlation function  $M_{cc}$  between the two mechanical displacements  $x_1$  and  $x_2$  with different inter-cavity optical coupling strength  $\kappa$ ,

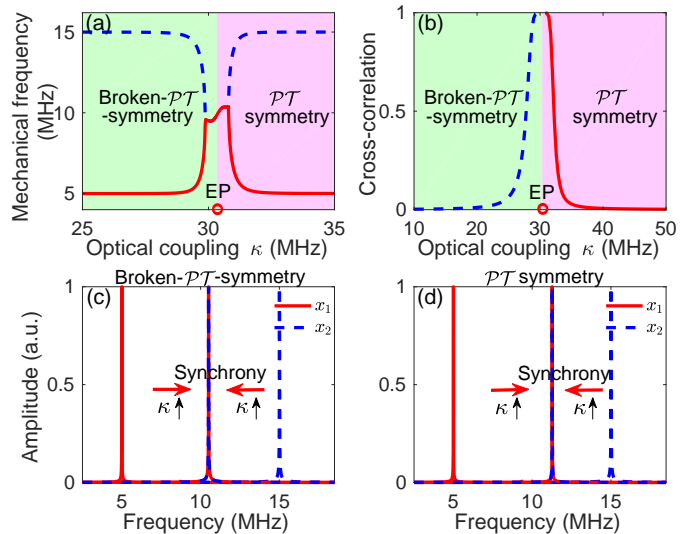


FIG. 4: (color online) (a) Effective mechanical frequencies  $\Omega_{1,\text{eff}}$  and  $\Omega_{2,\text{eff}}$  versus the optical coupling strength  $\kappa$ , where the red solid (blue dashed) curve represents the frequency of  $\beta_1$  ( $\beta_2$ ), the light green (pink) area is the broken- $\mathcal{PT}$ -symmetric ( $\mathcal{PT}$ -symmetric) regime. (b) Numerical results of cross-correlation  $M_{cc}$  with different values of  $\kappa$  in broken- $\mathcal{PT}$ -symmetric and  $\mathcal{PT}$ -symmetric regimes. (c) Spectrograms of mechanical modes  $x_1$  and  $x_2$  with increasing optical coupling strength  $\kappa$  in the broken- $\mathcal{PT}$ -symmetric regime. Here,  $\kappa \uparrow$  and  $\kappa \downarrow$  denote the increase and decrease of  $\kappa$ . (d) Spectrograms of mechanical modes  $x_1$  and  $x_2$  with decreasing optical coupling strength  $\kappa$  in the  $\mathcal{PT}$ -symmetric regime, in which weaker coupling strength  $\kappa$  makes the two resonators more easily to be synchronized.

where  $M_{cc}$  is defined as [47–52]

$$M_{cc} = \max_{0 < t < +\infty} \frac{1}{\sqrt{\phi_1 \phi_2}} \int_0^{+\infty} x_1(\tau - t) x_2(\tau) d\tau,$$

$$\phi_i = \int_0^{+\infty} x_i^2(\tau) d\tau. \quad (5)$$

This normalized cross-correlation function varies between 0 and 1. The maximum value of  $M_{cc} = 1$  indicates that the two time series of the mechanical displacements  $x_1$  and  $x_2$  have the exact same shape, even though their amplitudes may be different, which implies that the two self-sustained oscillators have the same frequency, that is, the onset of synchronization. As shown in Fig. 4(b), in the  $\mathcal{PT}$ -symmetric regime, smaller  $\kappa$  induces higher value of  $M_{cc}$  (the red solid curve), and  $M_{cc}$  reaches the maximum value (the unit) as  $\kappa$  decreases and approaches EP, which means that the two mechanical displacements  $x_1$  and  $x_2$  tend to be synchronized with the decrease of the inter-cavity coupling strength. However, in the broken- $\mathcal{PT}$  symmetric regime (the blue dashed curve), the cross-correlation function increases and tends to unit with the increase of  $\kappa$ , which means that stronger inter-cavity coupling strength will be helpful for synchronization as we expect.

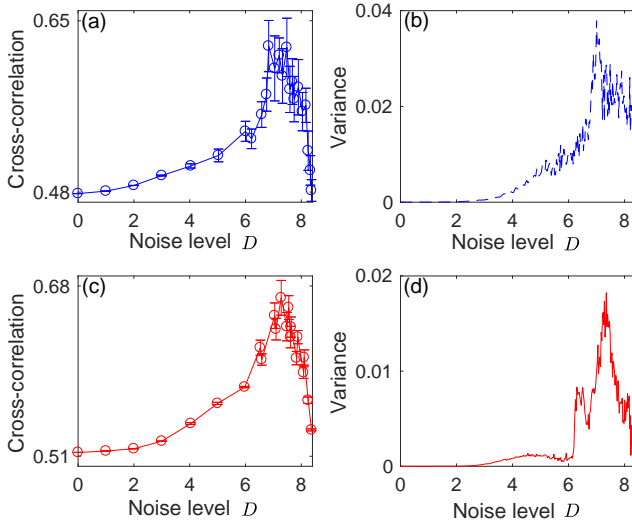


FIG. 5: (color online) (a) Effects of the stochastic noises on  $M_{cc}$  with respect to different stochastic noise intensity  $D$  in broken  $\mathcal{PT}$ -symmetric regime with  $\kappa = 27.76$  MHz. (b) Variances of  $M_{cc}$  versus noise level  $D$  in (a). (c) Effects of the stochastic noises on  $M_{cc}$  versus different  $D$  in  $\mathcal{PT}$ -symmetric regime with  $\kappa = 32.19$  MHz. The variance of  $M_{cc}$  is presented in (d).

#### IV. NOISE-ENHANCED SYNCHRONIZATION IN $\mathcal{PT}$ -SYMMETRIC OPTOMECHANICAL SYSTEM

##### A. Stochastic noises in the optical modes

We now study the effects of the stochastic noises on our  $\mathcal{PT}$ -symmetric system. Two independently-identically-distributed Gaussian white noises  $\xi_{1,2}$  are introduced for the two optical modes  $\alpha_{1,2}$ , such that  $\langle \xi_i(t) \xi_j(t+\tau) \rangle = 2D\delta_{ij}\delta(\tau)$ , where  $D$  is the intensity of the noises. Here, we have included the shifts of damping rates induced by stochastic noises into the gain ( $\gamma_1$ ) and loss ( $\gamma_2$ ) rates in our optomechanical system. Thus the dynamical equations of our  $\mathcal{PT}$ -symmetric system can be reexpressed as

$$\begin{aligned} \dot{\alpha}_1 &= i(\Delta_1 + g_{om}x_1)\alpha_1 + \gamma_1\alpha_1 - i\kappa\alpha_2 + \sqrt{2\gamma_{1ex}}\epsilon_1 \\ &\quad + \xi_1(t), \\ \dot{\alpha}_2 &= i(\Delta_2 + g_{om}x_2)\alpha_2 - \gamma_2\alpha_2 - i\kappa\alpha_1 + \sqrt{2\gamma_{2ex}}\epsilon_2 \\ &\quad + \xi_2(t), \\ \ddot{x}_1 &= -2\Gamma_{m1}\dot{x}_1 - \Omega_1^2x_1 - g_{om}|\alpha_1|^2, \\ \ddot{x}_2 &= -2\Gamma_{m2}\dot{x}_2 - \Omega_2^2x_2 - g_{om}|\alpha_2|^2. \end{aligned} \quad (6)$$

We present the numerical results of the cross-correlation function  $M_{cc}$  between the two mechanical oscillators in Figs. 5(a) and (c) by changing the noise strength  $D$  and fixing other parameters both in broken- $\mathcal{PT}$ -symmetric and  $\mathcal{PT}$ -symmetric regimes. It can be seen that  $M_{cc}$  is enhanced with increasing noise intensity  $D$  both in broken- $\mathcal{PT}$ -symmetric and  $\mathcal{PT}$ -symmetric

regime, reaches the maximal values at particular noise level, and then decreases at higher noise intensity. It means that synchronization process may benefit from noises [53–60] in our optomechanical  $\mathcal{PT}$ -symmetric system. To interpret what we observe, we can see that the noise will randomly shift the frequencies of the mechanical modes, especially when we approach the EP where the effects of noise are enhanced [61–64]. Since the frequencies of the two mechanical modes are far-separated, these random frequency shifts may decrease the difference between the frequencies of the two mechanical modes in a certain probability with increasing noise strength  $D$ , and thus increase the cross-correlation function  $M_{cc}$ . When we increase the noise strength  $D$  further, the noise will be strong enough to destroy the periodic oscillation of single mechanical oscillator and the  $\mathcal{PT}$ -symmetric structure of the optomechanical system, and thus decrease the degree of synchronization between the two mechanical oscillators. This interpretation can also be confirmed by checking the variance of  $M_{cc}$  versus the noise strength  $D$  (Fig. 5(b) and (d)). The variance of  $M_{cc}$  first increases with increasing noise strength  $D$  (note that  $M_{cc}$  increases at the same time), which means that more noises enter the system although  $M_{cc}$  is increased. The variance of  $M_{cc}$  then decreases when we increase  $D$  further, because the value of  $M_{cc}$  is too small in this case and the noise-induced fluctuations in  $M_{cc}$  are suppressed.

To give more insights for synchronization with optically stochastic noises in our  $\mathcal{PT}$ -symmetric optomechanical system, we show additional analysis of another index of synchronization—the Kramers rate, which is more suitable to describe noisy synchronized systems. The Kramers rates of two subsystems are alternative indices to show the correlation between two subsystems. When the Kramers rates of two subsystems coincide with each other, the two subsystems are well correlated [53]. We then calculate the Kramers rates  $r_1$  and  $r_2$  of the mechanical displacements  $x_1$  and  $x_2$ , respectively. The Kramers rate is originally defined as the transition rate between neighboring potential wells of a particle caused by stochastic forces, which was first proposed by Kramers in 1940 [65].

Here, we use the mean first passage time [66, 67], i.e., the average time that the particle moves from one potential well to the other well, to evaluate the Kramers rates  $r_1$  and  $r_2$  of mechanical displacements  $x_1$  and  $x_2$ . We obtain the histograms of  $x_{1,2}$  through numerical simulation first, and then find out the locations of the maximum probability of  $x_{1,2}$ , i.e., the potential wells of  $x_{1,2}$ , based on the distribution of histograms, by which we can obtain the mean first passage times  $\tau_{1,2}$ , i.e., the average value of the time intervals between two potential wells for each mechanical displacement. The Kramers rates  $r_1$  and  $r_2$  can then be calculated by the reciprocal of the mean first passage times  $\tau_{1,2}$ , i.e.,  $r_i = 1/\tau_i$  ( $i = 1, 2$ ). The simulation results for  $r_1$  and  $r_2$  are presented in Fig. 6. It can be seen that, both in broken- $\mathcal{PT}$ -symmetric (Fig. 6(a)) and  $\mathcal{PT}$ -symmetric (Fig. 6(b))

regimes, the Kramers rates  $r_1$  and  $r_2$  get closer with the increase of the noise intensity, which means that the partial frequencies of the mechanical displacements  $x_1$  and  $x_2$  get closer when the noise intensity  $D$  is increased. It means that the optically stochastic noises can improve the correlation between  $x_1$  and  $x_2$ .

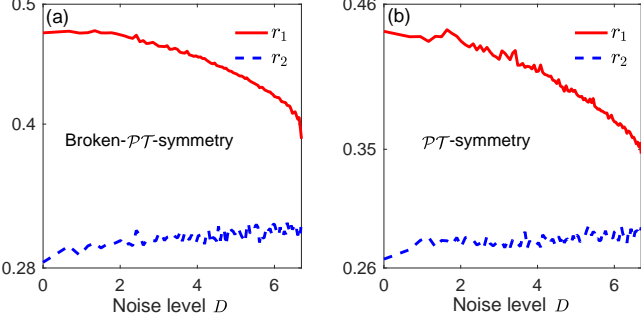


FIG. 6: (Color online) The Kramers rates  $r_1$  and  $r_2$  of mechanical displacements  $x_1$  and  $x_2$  versus the noise intensity  $D$  in broken- $\mathcal{PT}$ -symmetric and  $\mathcal{PT}$ -symmetric regime. (a) The red solid curve (blue dashed curve) represents the curve for Kramers rate  $r_1$  ( $r_2$ ) versus the noise intensity  $D$  in the broken- $\mathcal{PT}$ -symmetric regime. Here the optical coupling strength  $\kappa = 27.76$  MHz is fixed. (b) The Kramers rates  $r_1$  and  $r_2$  with different stochastic noise intensity  $D$  correspond to the  $\mathcal{PT}$ -symmetric regime, where the optical coupling strength is fixed as  $\kappa = 32.19$  MHz.

### B. Thermal noises in the mechanical modes

In the above analysis we do not consider the effects of the thermal noises in the mechanical modes. Actually, these thermal noises in the mechanical modes can also benefit the synchronization between the two mechanical modes in our  $\mathcal{PT}$ -symmetric optomechanical system. In order to simplify our discussions, we only consider the thermal noises in the mechanical modes in this section, and assume that the thermal noises in the mechanical modes are white noises, based on which the Langevin equation of the mechanical modes can be expressed as

$$\begin{aligned}\ddot{x}_1 &= -2\Gamma_m \dot{x}_1 - \tilde{\Omega}_1^2 x_1 - \kappa_{\text{mech}} x_2 + \Gamma_{\text{noise1}}(t), \\ \ddot{x}_2 &= -2\Gamma_m \dot{x}_2 - \tilde{\Omega}_2^2 x_2 - \kappa_{\text{mech}} x_1 + \Gamma_{\text{noise2}}(t),\end{aligned}\quad (7)$$

where the constant driving terms induced by optical modes have been included into  $x_{1,2}$  by a coordinate transformation for simplicity. The mechanical damping rate  $\Gamma_m$  includes the damping rate shift  $\delta\Gamma_m$  induced by the corresponding thermal noise, i.e.,  $\Gamma_m = \Gamma_{\text{mo}} + \delta\Gamma_m$ , where  $\Gamma_{\text{mo}}$  is the original mechanical damping rate without considering thermal noise. The mechanical thermal noises  $\Gamma_{\text{noise1}}$  and  $\Gamma_{\text{noise2}}$  are diffusion terms with  $\delta$ -correlated Gaussian distribution

$$\begin{aligned}\langle \Gamma_{\text{noise i}}(t) \rangle &= 0, \\ \langle \Gamma_{\text{noise i}}(t) \Gamma_{\text{noise j}}(t') \rangle &= 4\Gamma_m kT \delta(t - t'),\end{aligned}\quad (8)$$

where  $k$  is the Boltzman's constant and  $T$  is the temperature.

To show the positive influence of thermal noises on the synchronization, we present the numerical results of the normalized correlation function  $R$  [68] between the two mechanical oscillators in Figs. 7(a) and (b) by changing the temperature  $T$  and fixing other parameters in both broken- $\mathcal{PT}$ -symmetric and  $\mathcal{PT}$ -symmetric regimes, where  $T_r$  is the room temperature. In the broken- $\mathcal{PT}$ -symmetric regime with optical coupling strength  $\kappa = 27.76$  MHz,  $R$  (blue-dashed curve) is enhanced with increasing temperature  $T$ , and reaches 0.61 at the room temperature  $T_r$ , which is larger than 0.48 when we ignore the thermal noises. Similarly, in the  $\mathcal{PT}$ -symmetric regime with optical coupling strength  $\kappa = 32.19$  MHz,  $R$  (red-solid curve) increases with temperature  $T$ , and reaches 0.65 at the room temperature, which is larger than 0.51 when we ignore the thermal noises. It means that the thermal noises in the mechanical modes can also benefit the synchronization between the two mechanical modes in our optomechanical  $\mathcal{PT}$ -symmetric system.

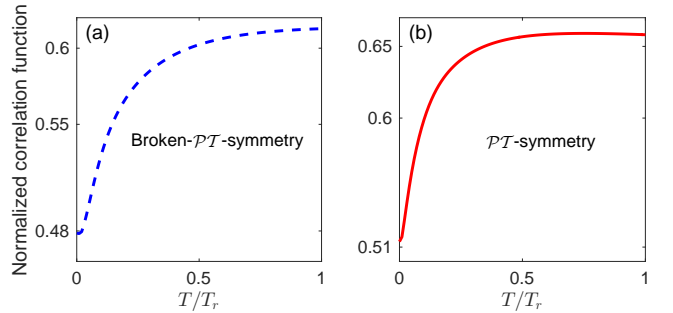


FIG. 7: (Color online) Numerical results of the normalized correlation function  $R$  with different values of temperature  $T$  in broken- $\mathcal{PT}$ -symmetric and  $\mathcal{PT}$ -symmetric regimes, where  $T_r$  denotes the room temperature. (a) Effects of the thermal noises on  $R$  with respect to different temperature  $T$  in broken- $\mathcal{PT}$ -symmetric regime with  $\kappa = 27.76$  MHz. (b) Effects of the thermal noises on  $R$  versus different  $T$  in  $\mathcal{PT}$ -symmetric regime with  $\kappa = 32.19$  MHz.

To give more insights into the phenomenon presented, we calculate the Kramers rates  $r_1$  and  $r_2$  of mechanical displacements  $x_1$  and  $x_2$ . The simulation results for Kramers rates  $r_1$  and  $r_2$  are shown in Figs. 8(a) and (b). In Fig. 8(a), the red solid curve denotes Kramers rate  $r_1$  with different values of temperature  $T$  in the broken- $\mathcal{PT}$ -symmetric regime with optical coupling strength  $\kappa = 27.76$  MHz, and the blue dashed curve corresponds to the Kramers rate  $r_2$ . We can see in Fig. 8(a) that Kramers rates  $r_1$  and  $r_2$  tend to get closer to each other as the temperature  $T$  increases to the room temperature  $T_r$ . Similar phenomenon can be observed in the  $\mathcal{PT}$ -symmetric regime as shown in Fig. 8(b), i.e., the mechanical thermal noises tend to decrease the difference between the Kramers rates  $r_1$  and  $r_2$  as the temperature increases to the room temperature, where the opti-

cal coupling strength is fixed as  $\kappa = 32.19$  MHz. These simulation results indicate that more mechanical thermal noises can lead the partial frequencies of the two mechanical displacements  $x_1$  and  $x_2$  to tend to be consistent with each other, and thus benefit the synchronization in our  $\mathcal{PT}$ -symmetric optomechanical system.

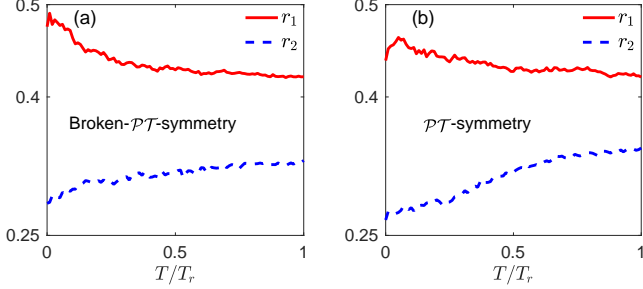


FIG. 8: (Color online) The Kramers rates  $r_1$  and  $r_2$  of mechanical displacements  $x_1$  and  $x_2$  versus the temperature  $T$  in both broken- $\mathcal{PT}$ -symmetric and  $\mathcal{PT}$ -symmetric regime, where  $T_r$  is the room temperature. (a) The red solid curve (blue dashed curve) denotes the Kramers rate  $r_1$  ( $r_2$ ) with increasing the temperature  $T$  in the broken- $\mathcal{PT}$ -symmetric regime, where the optical coupling strength  $\kappa = 27.76$  MHz is fixed. (b) The Kramers rates  $r_1$  and  $r_2$  versus the temperature  $T$  correspond to the  $\mathcal{PT}$ -symmetric regime ( $\kappa = 32.19$  MHz).

Furthermore, we can also observe the beneficial effect of the mechanical thermal noises on the synchronization by theoretically analyzing the correlation function between the two mechanical modes, when we consider small time  $t$ . Actually, at small time limit [68], the normalized correlation function between the two mechanical modes can be approximated as (see the derivations in Appendix G)

$$\begin{aligned} R(\tau, t) &\approx 1 - 2\tilde{\Omega}_1^2\tau t + \frac{q}{2}\kappa_{\text{mech}}\tilde{\Omega}_1^2\tau^2 t^2 + \frac{q}{3}\kappa_{\text{mech}}\tilde{\Omega}_1^2\tau^3 t^3 \\ &= 1 - 2\tilde{\Omega}_1^2\tau t + 2\Gamma_m k T \kappa_{\text{mech}} \tilde{\Omega}_1^2 \tau^2 t^2 \\ &\quad + \frac{4}{3}\Gamma_m k T \kappa_{\text{mech}} \tilde{\Omega}_1^2 \tau^3 t^3, \end{aligned} \quad (9)$$

where  $q$  is the intensity of the mechanical thermal noises, i.e.,  $q = 4\Gamma_m k T$ . It is shown in Eq. (9) that the normalized correlation function  $R$  can be enhanced by the increase of the intensity of the thermal noises, which is in consonance with the above simulation results, as shown in Figs. 7 and 8. It proves that the thermal noises in the mechanical modes can benefit the synchronization in our  $\mathcal{PT}$ -symmetric synchronization system.

## V. CONCLUSION AND DISCUSSION

We have shown that the mechanical motions of two coupled  $\mathcal{PT}$ -symmetric optomechanical resonators with far-off-resonant mechanical frequencies can be synchro-

nized when the system approaches the EP. In particular, in the  $\mathcal{PT}$ -symmetric regime, the two mechanical modes are easier to be synchronized with weaker optical coupling strength between the two optomechanical resonators. Additionally, it is shown that noises will be enhanced in the vicinity of the EP in our system, and the enhanced noises will benefit the synchronization process if only the strengths of the noises are not too strong. Our study opens up a new dimension of research for  $\mathcal{PT}$ -symmetric optomechanical system for possible applications such as metrology, cooling, and communication. It also gives new perspectives for synchronization in optomechanical systems.

## VI. ACKNOWLEDGMENTS

JZ is supported by the NSFC under Grant Nos. 61622306, 11674194. YXL and JZ are supported by the National Basic Research Program of China (973 Program) under Grant No. 2014CB921401, the Tsinghua University Initiative Scientific Research Program, and the Tsinghua National Laboratory for Information Science and Technology (TNList) Cross-discipline Foundation. JZ is also supported by the Youth Innovation Fund of Beijing National Research Center for Information Science and Technology (BNRist). LY is supported by the NSF grant No. EFMA1641109, ARO grant No. W911NF1210026 and ARO grant No. W911NF1710189.

## Appendix A: Weaker condition of $\mathcal{PT}$ -symmetry with $\Delta_1 \neq \Delta_2$

Generally, in our optomechanical system if we consider symmetric optical driving detunings  $\Delta_1 = \Delta_2$ , there exists an exceptional point where the two optical supermodes degenerate with each other at this point. However, if  $\Delta_- = |\Delta_2 - \Delta_1| \neq 0$ , the degeneracy of the optical supermodes at the previous exceptional point will be broken. Now we prove that even though the two optical driving detunings are asymmetric, i.e.,  $\Delta_- \neq 0$ , the non-degeneracy can be small enough that the characteristic of  $\mathcal{PT}$ -symmetry can still be maintained under a weaker condition, i.e.,  $\Delta_-$  is small enough.

In order to analyze the  $\mathcal{PT}$ -symmetric structure in our optomechanical system, we consider the optical modes only and assume that the nonlinear optomechanical interaction between the optical mode and mechanical mode is a nonlinearly induced frequency shift for the corresponding optical mode in each cavity [19]. Here, we treat the stationary state  $\beta_{1s}$  ( $\beta_{2s}$ ) of the mechanical mode  $\beta_1$  ( $\beta_2$ ) as a parameter which leads to a frequency detuning  $\Delta_{1s} = g_{om}(\beta_{1s} + \beta_{1s}^*)$  ( $\Delta_{2s} = g_{om}(\beta_{2s} + \beta_{2s}^*)$ ) for the optical mode  $\alpha_1$  ( $\alpha_2$ ). By taking  $\dot{\alpha}_{1,2} = \dot{\beta}_{1,2} = 0$  in Eqs. 1, we can obtain the stationary states of the optical and

mechanical modes which satisfies the following equations

$$\begin{aligned} 0 &= (\gamma_1 - i\Delta_1)\alpha_{1s} - i\kappa\alpha_{2s} - ig_{om}\alpha_{1s}(\beta_{1s} + \beta_{1s}^*) \\ &\quad + \sqrt{2\gamma_{1ex}}\epsilon_1, \\ 0 &= -(\gamma_2 + i\Delta_2)\alpha_{2s} - i\kappa\alpha_{1s} - ig_{om}\alpha_{2s}(\beta_{2s} + \beta_{2s}^*) \\ &\quad + \sqrt{2\gamma_{2ex}}\epsilon_2, \\ 0 &= -(\Gamma_{m1} + i\Omega_1)\beta_{1s} - ig_{om}|\alpha_{1s}|^2, \\ 0 &= -(\Gamma_{m2} + i\Omega_2)\beta_{2s} - ig_{om}|\alpha_{2s}|^2. \end{aligned} \quad (\text{A1})$$

By solving the above the equation, the stationary states of the mechanical modes can be expressed as

$$\begin{aligned} \beta_{1s} &= -g_{om}\frac{\Omega_1 + i\Gamma_{m1}}{\Gamma_{m1}^2 + \Omega_1^2}|\alpha_{1s}|^2, \\ \beta_{2s} &= -g_{om}\frac{\Omega_2 + i\Gamma_{m2}}{\Gamma_{m2}^2 + \Omega_2^2}|\alpha_{2s}|^2, \end{aligned} \quad (\text{A2})$$

and the stationary states of the optical modes satisfy the following equations

$$\begin{aligned} [\gamma_1 - i(\Delta_1 + \Delta_{1s})]\alpha_{1s} - i\kappa\alpha_{2s} + \sqrt{2\gamma_{1ex}}\epsilon_1 &= 0, \\ [-\gamma_2 - i(\Delta_2 + \Delta_{2s})]\alpha_{2s} - i\kappa\alpha_{1s} + \sqrt{2\gamma_{2ex}}\epsilon_2 &= 0, \end{aligned} \quad (\text{A3})$$

where

$$\begin{aligned} \Delta_{1s} &= -\frac{2\Omega_1 g_{om}^2}{\Gamma_{m1}^2 + \Omega_1^2}|\alpha_{1s}|^2, \\ \Delta_{2s} &= -\frac{2\Omega_2 g_{om}^2}{\Gamma_{m2}^2 + \Omega_2^2}|\alpha_{2s}|^2. \end{aligned} \quad (\text{A4})$$

By substituting the stationary states  $\beta_{1s}$  and  $\beta_{2s}$  into Eq. (1) and eliminating the mechanical modes, we have

$$\begin{aligned} \dot{\alpha}_1 &= [\gamma_1 - i(\Delta_1 + \Delta_{1s})]\alpha_1 - i\kappa\alpha_2 + \sqrt{2\gamma_{1ex}}\epsilon_1, \\ \dot{\alpha}_2 &= [-\gamma_2 - i(\Delta_2 + \Delta_{2s})]\alpha_2 - i\kappa\alpha_1 + \sqrt{2\gamma_{2ex}}\epsilon_2. \end{aligned} \quad (\text{A5})$$

Based on Eq. (A5), we can calculate the eigenfrequencies of the optical supermodes as

$$\begin{aligned} \omega_{o+} &= \frac{\gamma_1 - \gamma_2}{2} - i\frac{\Delta_1 + \Delta_{1s} + \Delta_2 + \Delta_{2s}}{2} \\ &\quad + \sqrt{\left[\frac{\gamma_1 + \gamma_2}{2} + i\left(\frac{\Delta_2 + \Delta_{2s}}{2} - \frac{\Delta_1 + \Delta_{1s}}{2}\right)\right]^2 - \kappa^2}, \\ \omega_{o-} &= \frac{\gamma_1 - \gamma_2}{2} - i\frac{\Delta_1 + \Delta_{1s} + \Delta_2 + \Delta_{2s}}{2} \\ &\quad - \sqrt{\left[\frac{\gamma_1 + \gamma_2}{2} + i\left(\frac{\Delta_2 + \Delta_{2s}}{2} - \frac{\Delta_1 + \Delta_{1s}}{2}\right)\right]^2 - \kappa^2}. \end{aligned} \quad (\text{A6})$$

Considering the balanced gain and loss ( $\gamma_1 = \gamma_2 = \gamma$ ),

the above equations can be reduced to

$$\begin{aligned} \omega_{o+} &= -i\frac{\Delta_1 + \Delta_{1s} + \Delta_2 + \Delta_{2s}}{2} \\ &\quad + \sqrt{\left[\gamma + i\left(\frac{\Delta_2 + \Delta_{2s}}{2} - \frac{\Delta_1 + \Delta_{1s}}{2}\right)\right]^2 - \kappa^2}, \\ \omega_{o-} &= -i\frac{\Delta_1 + \Delta_{1s} + \Delta_2 + \Delta_{2s}}{2} \\ &\quad - \sqrt{\left[\gamma + i\left(\frac{\Delta_2 + \Delta_{2s}}{2} - \frac{\Delta_1 + \Delta_{1s}}{2}\right)\right]^2 - \kappa^2}. \end{aligned} \quad (\text{A7})$$

Actually, the vacuum optomechanical coupling  $g_{om}$  in general optical cavities [10] is very small, thus if  $\Delta_- = \Delta_2 - \Delta_1$  is small enough, the imaginary part in the root sign in Eq. A7 can be ignored, and the eigenvalues can be reduced to

$$\begin{aligned} \omega_{o+} &\approx -i\frac{\Delta_1 + \Delta_2}{2} + \sqrt{\gamma^2 - \kappa^2} \\ \omega_{o-} &\approx -i\frac{\Delta_1 + \Delta_2}{2} - \sqrt{\gamma^2 - \kappa^2}. \end{aligned} \quad (\text{A8})$$

It means that the two eigenvalues of optical supermodes tend to degenerate with each other at the exceptional point  $\kappa = \gamma$ . In fact, by substituting  $\alpha_{1s}$  and  $\alpha_{2s}$  into Eqs. A7, the non-degeneracy of the optical supermodes at the exceptional point ( $\kappa = \gamma$ ) can be evaluated as

$$\frac{\Delta_{\text{split}}}{\gamma} \approx \sqrt{\frac{\Delta_-^3}{\frac{2}{3}\gamma\left(g_{om}^2\frac{\Omega_2 + \Omega_1}{\Omega_1\Omega_2}\gamma\epsilon^2\right)^{2/3}}}, \quad (\text{A9})$$

thus when

$$g_{om} \ll \Delta_- \ll \sqrt[3]{\frac{2}{3}\gamma\left(g_{om}^2\frac{\Omega_2 + \Omega_1}{\Omega_1\Omega_2}\gamma\epsilon^2\right)^2} \ll \gamma, \quad (\text{A10})$$

where  $\Delta_{\text{split}} = \text{Im}[\omega_{o+} - \omega_{o-}] = \text{Re}[\omega_{o+} - \omega_{o-}]$ . It can be inferred that this non-degeneracy can be very small that the properties of  $\mathcal{PT}$ -symmetric structure can be greatly held in our optomechanical system. We name the condition of Eq. A10 as weaker condition for  $\mathcal{PT}$ -symmetry in our optomechanical system, and it can be easily realized in general cavity optomechanical systems.

As for the simulation results in Figs. 2 (a) and (b) in the main text, we first calculate the stationary states of  $\alpha_{1s}$  and  $\alpha_{2s}$  by numerically solving the Eqs. A3, then the eigenvalues of optical supermodes can be obtained by substituting  $\alpha_{1s}$  and  $\alpha_{2s}$  into Eqs. A7.

## Appendix B: The derivation of the reduced dynamical equation of the mechanical modes

Based on the dynamical equation in Eq. (1), we can adiabatically eliminate the degrees of freedom of the optical modes, and derive the reduced dynamical equations

of the mechanical modes. In fact, by rewriting the first two equations in Eq. (1) in matrix format, we have

$$\begin{bmatrix} \dot{\alpha}_1 \\ \dot{\alpha}_2 \end{bmatrix} = M \begin{bmatrix} \alpha_1 \\ \alpha_2 \end{bmatrix} + \begin{bmatrix} -ig_{om}\alpha_1(\beta_1 + \beta_1^*) \\ -ig_{om}\alpha_2(\beta_2 + \beta_2^*) \end{bmatrix} + \begin{bmatrix} \sqrt{2\gamma_{1ex}}\epsilon_1 \\ \sqrt{2\gamma_{2ex}}\epsilon_2 \end{bmatrix}, \quad (\text{B1})$$

where

$$M = \begin{bmatrix} \gamma_1 - i\Delta_1 & -i\kappa \\ -i\kappa & -\gamma_2 - i\Delta_2 \end{bmatrix}.$$

The matrix  $M$  can be diagonalized as

$$M = T\Lambda T^{-1},$$

where

$$\Lambda = \begin{bmatrix} \omega_+ & 0 \\ 0 & \omega_- \end{bmatrix}, T = \begin{bmatrix} \tau_+ & \tau_- \\ 1 & 1 \end{bmatrix},$$

and

$$\begin{aligned} \omega_+ &= \frac{\gamma_1 - \gamma_2}{2} - i\frac{\Delta_1 + \Delta_2}{2} \\ &\quad - i\sqrt{\kappa^2 + \left(\frac{\Delta_1 - \Delta_2}{2} + i\frac{\gamma_1 + \gamma_2}{2}\right)^2}, \\ \omega_- &= \frac{\gamma_1 - \gamma_2}{2} - i\frac{\Delta_1 + \Delta_2}{2} \\ &\quad + i\sqrt{\kappa^2 + \left(\frac{\Delta_1 - \Delta_2}{2} + i\frac{\gamma_1 + \gamma_2}{2}\right)^2}, \\ \tau_+ &= \frac{\Delta_1 - \Delta_2 + i(\gamma_1 + \gamma_2)}{2\kappa} \\ &\quad + \sqrt{1 + \left(\frac{\Delta_1 - \Delta_2 + i(\gamma_1 + \gamma_2)}{2\kappa}\right)^2}, \\ \tau_- &= \frac{\Delta_1 - \Delta_2 + i(\gamma_1 + \gamma_2)}{2\kappa} \\ &\quad - \sqrt{1 + \left(\frac{\Delta_1 - \Delta_2 + i(\gamma_1 + \gamma_2)}{2\kappa}\right)^2}. \end{aligned}$$

Thus, we can introduce the following optical supermodes

$$\begin{bmatrix} \alpha_+ \\ \alpha_- \end{bmatrix} = T^{-1} \begin{bmatrix} \alpha_1 \\ \alpha_2 \end{bmatrix}, \quad (\text{B2})$$

by which Eq. (B1) can be reexpressed as

$$\begin{bmatrix} \dot{\alpha}_+ \\ \dot{\alpha}_- \end{bmatrix} = \begin{bmatrix} \omega_+ & 0 \\ 0 & \omega_- \end{bmatrix} \begin{bmatrix} \alpha_+ \\ \alpha_- \end{bmatrix} - ig_{om} \times \begin{bmatrix} (\lambda_+\alpha_+ + \lambda_-\alpha_-)(\beta_1 + \beta_1^*) - \lambda_-(\alpha_+ + \alpha_-)(\beta_2 + \beta_2^*) \\ -(\lambda_+\alpha_+ + \lambda_-\alpha_-)(\beta_1 + \beta_1^*) + \lambda_+(\alpha_+ + \alpha_-)(\beta_2 + \beta_2^*) \end{bmatrix} + \begin{bmatrix} \mu\sqrt{2\gamma_{1ex}}\epsilon_1 - \lambda_-\sqrt{2\gamma_{2ex}}\epsilon_2 \\ -\mu\sqrt{2\gamma_{1ex}}\epsilon_1 + \lambda_+\sqrt{2\gamma_{2ex}}\epsilon_2 \end{bmatrix},$$

where

$$\begin{aligned} \lambda_- &= \frac{\Delta_1 - \Delta_2 + i(\gamma_1 + \gamma_2) - \Xi_1}{2\Xi_1}, \\ \lambda_+ &= \frac{\Delta_1 - \Delta_2 + i(\gamma_1 + \gamma_2) + \Xi_1}{2\Xi_1}, \\ \mu &= \frac{\kappa}{\Xi_1}, \end{aligned}$$

where

$$\Xi_1 = \sqrt{4\kappa^2 + (\Delta_1 - \Delta_2 + i(\gamma_1 + \gamma_2))^2}.$$

To adiabatically eliminate the degrees of freedom of the optical modes, we let  $\dot{\alpha}_+ = \dot{\alpha}_- = 0$ , by which we can obtain the following stationary solution

$$\begin{aligned} \alpha_{+ss} &= \frac{-\mu(\omega_- - ig_{om}(\beta_2 + \beta_2^*))\sqrt{2\gamma_{1ex}}\epsilon_1}{\Xi_2} \\ &\quad + \frac{\lambda_-(\omega_- - ig_{om}(\beta_1 + \beta_1^*))\sqrt{2\gamma_{2ex}}\epsilon_2}{\Xi_2}, \\ \alpha_{-ss} &= \frac{\mu(\omega_+ - ig_{om}(\beta_2 + \beta_2^*))\sqrt{2\gamma_{1ex}}\epsilon_1}{\Xi_2} \\ &\quad - \frac{\lambda_+(\omega_+ - ig_{om}(\beta_1 + \beta_1^*))\sqrt{2\gamma_{2ex}}\epsilon_2}{\Xi_2} \quad (\text{B3}) \end{aligned}$$

where

$$\begin{aligned} \Xi_2 &= \omega_+\omega_- + ig_{om}(\omega_+\lambda_- - \omega_-\lambda_+)(\beta_1 + \beta_1^*) \\ &\quad + ig_{om}(-\omega_+\lambda_+ + \omega_-\lambda_-)(\beta_2 + \beta_2^*) \\ &\quad - g_{om}^2(\lambda_+ - \lambda_-)^2(\beta_1 + \beta_1^*)(\beta_2 + \beta_2^*) \quad (\text{B4}) \end{aligned}$$

By introducing the power-series expansion and omitting high-order terms of  $\beta_1$  and  $\beta_2$  ( $g_{om} \ll |\Delta_2 - \Delta_1|$ ), the above solutions can be simplified as

$$\begin{aligned} \alpha_{+ss} &\approx -\frac{\mu\sqrt{2\gamma_{1ex}}\epsilon_1 - \lambda_-\sqrt{2\gamma_{2ex}}\epsilon_2}{\omega_+} \\ &\quad + ig_{om}\frac{\Xi_3 - \lambda_-\omega_+\omega_- \sqrt{2\gamma_{2ex}}\epsilon_2}{(\omega_+\omega_-)^2}(\beta_1 + \beta_1^*) \\ &\quad + ig_{om}\frac{-\Xi_3 + \mu\omega_+\omega_- \sqrt{2\gamma_{1ex}}\epsilon_1}{(\omega_+\omega_-)^2}(\beta_2 + \beta_2^*), \\ \alpha_{-ss} &\approx -\frac{\mu\sqrt{2\gamma_{1ex}}\epsilon_1 - \lambda_+\sqrt{2\gamma_{2ex}}\epsilon_2}{\omega_-} \\ &\quad + ig_{om}\frac{\Xi_4 - \lambda_+\omega_+\omega_- \sqrt{2\gamma_{2ex}}\epsilon_2}{(\omega_+\omega_-)^2}(\beta_1 + \beta_1^*) \\ &\quad + ig_{om}\frac{-\Xi_4 + \mu\omega_+\omega_- \sqrt{2\gamma_{1ex}}\epsilon_1}{(\omega_+\omega_-)^2}(\beta_2 + \beta_2^*), \quad (\text{B5}) \end{aligned}$$

where

$$\begin{aligned} \Xi_3 &= \omega_-\left(\mu\sqrt{2\gamma_{1ex}}\epsilon_1 - \lambda_-\sqrt{2\gamma_{2ex}}\epsilon_2\right)(\omega_+\lambda_- - \omega_-\lambda_+), \\ \Xi_4 &= \omega_+\left(\mu\sqrt{2\gamma_{1ex}}\epsilon_1 - \lambda_+\sqrt{2\gamma_{2ex}}\epsilon_2\right)(\omega_+\lambda_- - \omega_-\lambda_+). \end{aligned}$$

Thus, the stationary solutions of  $\alpha_1$  and  $\alpha_2$  can be expressed as

$$\begin{aligned}\alpha_{1ss} &= \tau_+ \alpha_{+ss} + \tau_- \alpha_{-ss} \\ &= \frac{\sigma_2 \sqrt{2\gamma_{1ex}} \epsilon_1 - i\kappa \sqrt{2\gamma_{2ex}} \epsilon_2}{\kappa^2 + \delta^2 + \sigma^2} \\ &\quad - ig_{om} \frac{\sigma_2^2 \sqrt{2\gamma_{1ex}} \epsilon_1 - i\kappa \sigma_2 \sqrt{2\gamma_{2ex}} \epsilon_2}{\kappa^2 + \delta^2 + \sigma^2} (\beta_1 + \beta_1^*) \\ &\quad + ig_{om} \frac{\kappa^2 \sqrt{2\gamma_{1ex}} \epsilon_1 + i\kappa \sigma_1 \sqrt{2\gamma_{2ex}} \epsilon_2}{\kappa^2 + \delta^2 + \sigma^2} (\beta_2 + \beta_2^*), \\ \alpha_{2ss} &= \alpha_{+ss} + \alpha_{-ss} \\ &= \frac{-i\kappa \sqrt{2\gamma_{1ex}} \epsilon_1 + \sigma_1 \sqrt{2\gamma_{2ex}} \epsilon_2}{\kappa^2 + \delta^2 + \sigma^2} \\ &\quad + ig_{om} \frac{i\kappa \sigma_2 \sqrt{2\gamma_{1ex}} \epsilon_1 + \kappa^2 \sqrt{2\gamma_{2ex}} \epsilon_2}{\kappa^2 + \delta^2 + \sigma^2} (\beta_1 + \beta_1^*) \\ &\quad - ig_{om} \frac{-i\kappa \sigma_1 \sqrt{2\gamma_{1ex}} \epsilon_1 + \sigma_1^2 \sqrt{2\gamma_{2ex}} \epsilon_2}{\kappa^2 + \delta^2 + \sigma^2} (\beta_2 + \beta_2^*),\end{aligned}\quad (B6)$$

where

$$\begin{aligned}\sigma_1 &= -\gamma_1 + i\Delta_1, \quad \sigma_2 = \gamma_2 + i\Delta_2, \\ \delta &= \frac{\Delta_1 - \Delta_2}{2} + i\frac{\gamma_1 + \gamma_2}{2}, \quad \sigma = \frac{-\gamma_1 + \gamma_2}{2} + i\frac{\Delta_1 + \Delta_2}{2}.\end{aligned}$$

By substituting the above stationary solution into the dynamical equations of the mechanical modes  $\beta_1$  and  $\beta_2$  in Eq. (1), and dropping the counter-rotating terms with  $\beta_{1,2}^*$ , the dynamical equation of reduced mechanical system can be expressed in the matrix format as

$$\begin{bmatrix} \dot{\beta}_1 \\ \dot{\beta}_2 \end{bmatrix} = \begin{bmatrix} -\Gamma_{m1} - i(\Omega_1 + \delta\Omega_1) & \kappa_{\text{mech}} \\ \kappa_{\text{mech}} & -\Gamma_{m2} - i(\Omega_2 + \delta\Omega_2) \end{bmatrix} \times \begin{bmatrix} \beta_1 \\ \beta_2 \end{bmatrix} - \begin{bmatrix} i\eta_1 \\ i\eta_2 \end{bmatrix}, \quad (B7)$$

where

$$\begin{aligned}\delta\Omega_1 &= \frac{4g_{om}^2 [(\kappa^2 - \Delta_1 \Delta_2) \Delta_2 - \Delta_1 \gamma_2^2]}{[(\kappa^2 - \Delta_1 \Delta_2 - \gamma_1 \gamma_2)^2 + (\Delta_1 \gamma_2 - \Delta_2 \gamma_1)^2]^2}, \\ &\quad \times [\gamma_2^2 \gamma_{1ex} \epsilon_1^2 + (\Delta_2 \sqrt{\gamma_{1ex}} \epsilon_1 - \kappa \sqrt{\gamma_{2ex}} \epsilon_2)^2],\end{aligned}$$

$$\begin{aligned}\delta\Omega_2 &= \frac{4g_{om}^2 [(\kappa^2 - \Delta_1 \Delta_2) \Delta_1 - \Delta_2 \gamma_1^2]}{[(\kappa^2 - \Delta_1 \Delta_2 - \gamma_1 \gamma_2)^2 + (\Delta_1 \gamma_2 - \Delta_2 \gamma_1)^2]^2}, \\ &\quad \times [\gamma_1^2 \gamma_{2ex} \epsilon_2^2 + (\kappa \sqrt{\gamma_{1ex}} \epsilon_1 - \Delta_1 \sqrt{\gamma_{2ex}} \epsilon_2)^2],\end{aligned}$$

$$\begin{aligned}\kappa_{\text{mech}} &= 4g_{om}^2 \kappa \times \\ &\quad \left[ \frac{\kappa \gamma_{1ex} \epsilon_1^2 [\Delta_2 (\kappa^2 - \Delta_1 \Delta_2 - 2\gamma_1 \gamma_2) + \Delta_1 \gamma_2^2]}{[(\kappa^2 - \Delta_1 \Delta_2 - \gamma_1 \gamma_2)^2 + (\Delta_1 \gamma_2 - \Delta_2 \gamma_1)^2]^2} \right. \\ &\quad + \frac{+\kappa \gamma_{2ex} \epsilon_2^2 [\Delta_1 (\kappa^2 - \Delta_1 \Delta_2) - \Delta_2 \gamma_1^2]}{[(\kappa^2 - \Delta_1 \Delta_2 - \gamma_1 \gamma_2)^2 + (\Delta_1 \gamma_2 - \Delta_2 \gamma_1)^2]^2} \\ &\quad - \frac{\sqrt{\gamma_{1ex} \gamma_{2ex}} \epsilon_1 \epsilon_2}{[(\kappa^2 - \Delta_1 \Delta_2 - \gamma_1 \gamma_2)^2 + (\Delta_1 \gamma_2 - \Delta_2 \gamma_1)^2]^2} \\ &\quad \left. \times [(\kappa^2 - \gamma_1 \gamma_2)^2 - \Delta_1^2 \Delta_2^2 - (\Delta_1^2 \gamma_2^2 - \Delta_2^2 \gamma_1^2)] \right].\end{aligned}\quad (B8)$$

$$\begin{aligned}\eta_1 &= \frac{g_{om} [\gamma_2^2 \epsilon_1^2 + (\Delta_2 \epsilon_1 - \kappa \epsilon_2)^2]}{(\kappa^2 - \Delta_1 \Delta_2 - \gamma_1 \gamma_2)^2 + (\Delta_1 \gamma_2 - \Delta_2 \gamma_1)^2}, \\ \eta_2 &= \frac{g_{om} [\gamma_1^2 \epsilon_2^2 + (\kappa \epsilon_1 - \Delta_1 \epsilon_2)^2]}{(\kappa^2 - \Delta_1 \Delta_2 - \gamma_1 \gamma_2)^2 + (\Delta_1 \gamma_2 - \Delta_2 \gamma_1)^2}.\end{aligned}\quad (B9)$$

### Appendix C: The optomechanics-induced effective mechanical frequency shifts and mechanical coupling

Let us assume that the gain and loss are well-balanced such that  $\gamma_1 = \gamma_2 \equiv \gamma$  and consider the critical coupling case such that  $\gamma_{1ex} = \gamma_{2ex} = \gamma/2$ . When  $g_{om} \ll |\Delta_1 - \Delta_2| \ll \kappa, \gamma$  (or Eq. A10) and  $\epsilon_1 = \epsilon_2 \equiv \epsilon$ , the two mechanical frequency shifts  $\delta\Omega_{1,2}$  in Eq. B8 can be simplified as

$$\delta\Omega_1 = -\delta\Omega_2 \approx \frac{g_{om}^2 \Delta_- (\gamma^2 + \kappa^2)^2 \gamma \epsilon^2}{[(\kappa^2 - \gamma^2)^2 + \gamma^2 \Delta_-^2]}, \quad (C1)$$

we show the optomechanics-induced mechanical frequency shifts  $\delta\Omega_{1,2}$  in Fig. 9 (a). When the system is far away from EP, the mechanical frequency shifts  $\delta\Omega_1$  (red solid line) and  $\delta\Omega_2$  (red dashed line) are very small, and can be omitted in comparison to the mechanical frequencies  $\Omega_{1,2}$ . However, both frequency shifts  $\delta\Omega_1$  and  $\delta\Omega_2$  will be greatly amplified in the vicinity of EP, which will modify the mechanical frequencies  $\Omega_{1,2}$  such that  $\Omega_1 + \delta\Omega_1 = \Omega_2 + \delta\Omega_2$ . As shown in Fig. 9 (a), in the  $\mathcal{PT}$ -symmetric regime of the optical modes, these mechanical frequency shifts are enhanced with the decrease of the optical coupling strength  $\kappa$ , which means that smaller coupling strength  $\kappa$  between two optical modes is better for synchronization. In addition, as shown in Fig. 9 (a), the difference between the detuning frequencies of the two optical modes, i.e.,  $|\Delta_2 - \Delta_1|$ , significantly influences the amplification effects of the mechanical frequency shifts  $\delta\Omega_{1,2}$  when the system is around EP. By fixing  $\Delta_2 = 5$  MHz, we plot the curves of  $\delta\Omega_{1,2}$  for different  $\Delta_1$ . We can see that the mechanical frequency shifts  $\delta\Omega_{1,2}$  are greatly enhanced with the decrease of  $|\Delta_2 - \Delta_1|$  in the vicinity of EP.

Under the same assumptions, the strength of the effective mechanical coupling in Eq. B8 can be simplified as

$$\kappa_{\text{mech}} \approx \frac{4g_{om}^2 \Delta_- \kappa^2 \gamma^3 \epsilon^2}{[(\kappa^2 - \gamma^2)^2 + \gamma^2 \Delta_-^2]}, \quad (C2)$$

and thus the effective mechanical coupling will be greatly amplified in the vicinity of EP. We then plot the curves of the effective mechanical coupling strength  $\kappa_{\text{mech}}$  versus the optical coupling strength  $\kappa$  in Fig. 9 (b). Here we also fix  $\Delta_2 = 5$  MHz and tune the detuning frequency  $\Delta_1$ . It can be seen that the effective mechanical coupling strength  $\kappa_{\text{mech}}$  is significantly enhanced in the vicinity of EP. Therefore, in the  $\mathcal{PT}$ -symmetric regime of the optical modes, weaker optical coupling strength leads to stronger effective mechanical coupling strength, and thus

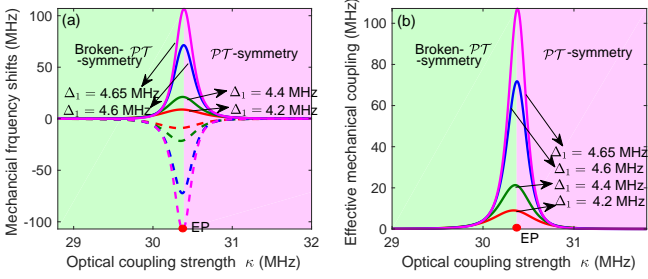


FIG. 9: (Color online) (a) The optomechanics-induced mechanical frequency shifts  $\delta\Omega_{1,2}$  versus the optical coupling strength  $\kappa$  in the broken- $\mathcal{PT}$ -symmetric regime (light green area) and  $\mathcal{PT}$ -symmetric regime (pink area). Here, we fix  $\Delta_2 = 5$  MHz and plot the curves of  $\delta\Omega_{1,2}$  for different  $\Delta_1$ . The solid (dashed) curves denote the curves of the mechanical frequency shift  $\delta\Omega_1$  ( $\delta\Omega_2$ ) with different  $\Delta_1$ . (b) The effective mechanical coupling strength  $\kappa_{\text{mech}}$  between the two mechanical modes versus the optical coupling strength  $\kappa$ .

may be helpful for the synchronization between the two mechanical modes. It is also shown that the degree of amplification of  $\kappa_{\text{mech}}$  is extensively enhanced with the decreasing of  $|\Delta_2 - \Delta_1|$  in the vicinity of EP.

#### Appendix D: The influence of the effective mechanical coupling on synchronization

In this part we discuss the positive effect of the enhancement of the effective mechanical coupling  $\kappa_{\text{mech}}$  on the synchronization between mechanical modes, i.e., the stronger the  $\kappa_{\text{mech}}$  is, the easier the synchronization is. For simplicity and clarity, we re-express the dynamical equation in Eq. (B7) by using the differential operator format as follows

$$[\mathcal{D} + (\Gamma_{m1} + i(\Omega_1 + \delta\Omega_1))] \beta_1 + \kappa_{\text{mech}} \beta_2 = -i\eta_1, \\ \kappa_{\text{mech}} \beta_1 + [\mathcal{D} + (\Gamma_{m2} + i(\Omega_2 + \delta\Omega_2))] \beta_2 = -i\eta_2,$$

where  $\mathcal{D}$  represents the differential operator. By eliminating the degree of freedom of  $\beta_2$ , we can derive the dynamical equation of  $\beta_1$ , and then obtain the characteristic equation of this coupled system as follows

$$\lambda^2 + [\Gamma_{m1} + \Gamma_{m2} + i(\Omega_1 + \delta\Omega_1 + \Omega_2 + \delta\Omega_2)] \lambda \\ + [\Gamma_{m1} + i(\Omega_1 + \delta\Omega_1)] [\Gamma_{m2} + i(\Omega_2 + \delta\Omega_2)] - \kappa_{\text{mech}}^2 = 0.$$

By considering  $\Gamma_{m1} = \Gamma_{m2} = \Gamma_m$ , the roots of this characteristic equation can be expressed as

$$\lambda_+ = -\Gamma_m - i\Omega_{\text{Ave}+} + i\sqrt{\Omega_{\text{Ave}-}^2 - \kappa_{\text{mech}}^2}, \\ \lambda_- = -\Gamma_m - i\Omega_{\text{Ave}+} - i\sqrt{\Omega_{\text{Ave}-}^2 - \kappa_{\text{mech}}^2}, \quad (\text{D1})$$

where

$$\Omega_{\text{Ave}+} = \frac{\Omega_1 + \delta\Omega_1 + \Omega_2 + \delta\Omega_2}{2}, \\ \Omega_{\text{Ave}-} = \frac{\Omega_1 + \delta\Omega_1 - \Omega_2 - \delta\Omega_2}{2}.$$

It can be easily seen that in the weak coupling regime such that  $\kappa_{\text{mech}} < \Omega_{\text{Ave}-}$ , the vibration frequencies of the mechanical modes  $\beta_{1,2}$  are close to each other with the increase of the effective coupling strength  $\kappa_{\text{mech}}$ , which means that the degree of synchronization between the two mechanical modes increases with the increase of  $\kappa_{\text{mech}}$ . At the critical point such that  $\kappa_{\text{mech}} = \Omega_{\text{Ave}-}$ , the two oscillators will have the same vibration frequency  $\Omega_{\text{Ave}+}$ , which means that these two mechanical modes are with frequency synchronization, i.e., the frequencies of the two mechanical modes are equal to each other. It is shown that a stronger effective mechanical coupling strength can improve the degree of the synchronization between mechanical modes in our system, and finally leads to the frequency synchronization when the effective mechanical coupling is strong enough.

In addition, in the weak coupling regime, the Eq. (D1) can also be re-expressed as

$$\lambda_+ = \Gamma_m - i(\Omega_2 + \delta\Omega_2 - \delta\Omega_{\text{coup}}) \\ \lambda_- = \Gamma_m - i(\Omega_1 + \delta\Omega_1 + \delta\Omega_{\text{coup}}), \quad (\text{D2})$$

where

$$\delta\Omega_{\text{coup}} = \frac{\Omega_2 + \delta\Omega_2 - \Omega_1 - \delta\Omega_1}{2} \\ - \sqrt{\left(\frac{\Omega_2 + \delta\Omega_2 - \Omega_1 - \delta\Omega_1}{2}\right)^2 - \kappa_{\text{mech}}^2} \quad (\text{D3})$$

is induced by the effective mechanical coupling strength  $\kappa_{\text{mech}}$ . It can be seen in Eq. (D2) that both optomechanics-induced mechanical frequency shift  $\delta\Omega_i$  and effective mechanical coupling  $\kappa_{\text{mech}}$  can lead to frequency shifts of the two mechanical modes, and thus contribute to the synchronization together.

#### Appendix E: The enhancement of the effective optomechanical interaction

In our  $\mathcal{PT}$ -symmetric optomechanical system, there exists an enhancement of the effective optomechanical interaction due to the topological-singularity-induced amplification of optomechanical nonlinearity in the vicinity of the exceptional point [18, 64]. This enhanced optomechanical interaction then leads to the amplifications of the optomechanics-induced mechanical frequency shifts  $\delta\Omega_{1,2}$  and the effective mechanical coupling strength  $\kappa_{\text{mech}}$ . Since both the optomechanics-induced mechanical frequency shifts and the effective mechanical coupling can change the frequency of the two mechanical modes, thus the synchronization between far-off-resonant mechanical modes can be realized with sufficiently large optomechanical interaction strength. In the  $\mathcal{PT}$ -symmetric regime, the system approaches to the exceptional point with the decrease of optical coupling strength  $\kappa$ , which results in an enhancement of the optomechanical coupling and

thus compensates the reduction of the optical coupling strength. In the following part of this subsection, we will discuss this enhanced effective optomechanical interaction in our  $\mathcal{PT}$ -symmetric optomechanical system.

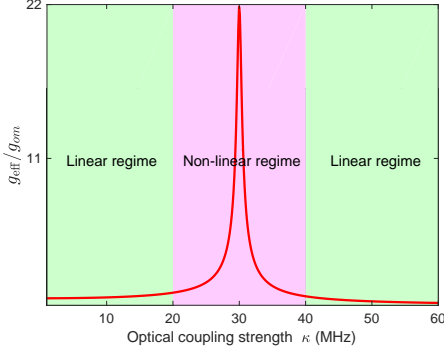


FIG. 10: (Color online) Effective optomechanical coupling strength  $g_{\text{eff}}$  versus the optical coupling strength  $\kappa$ . In the green area, the system is far away from EP, and the effective optomechanical coupling strength  $g_{\text{eff}}$  is linearly dependent on  $\kappa$ . In the pink area, the system is in the vicinity of EP, and in this case,  $g_{\text{eff}}$  changes nonlinearly with  $\kappa$ .

In our optomechanical system, the interaction Hamiltonian between optical modes and mechanical modes can be expressed as

$$H_{\text{int}} = g_{\text{om}} a_1^\dagger a_1 (b_1^\dagger + b_1) + g_{\text{om}} a_2^\dagger a_2 (b_2^\dagger + b_2), \quad (\text{E1})$$

where  $a_1$  ( $a_2$ ) and  $b_1$  ( $b_2$ ) represent the annihilation operator of the optical mode and mechanical mode in the active (passive) resonator, respectively, and  $g_{\text{om}}$  is the optomechanical coupling strength. If we re-write this interaction Hamiltonian  $H_{\text{int}}$  in the optical supermodes picture, then the effective optomechanical coupling strength  $g_{\text{eff}}$  between optical supermodes and mechanical modes can be expressed as

$$g_{\text{eff}} \approx \frac{g_{\text{om}}}{2} \frac{\gamma^2 + \sqrt{(\kappa^2 - \gamma^2)^2 + \gamma^2 \Delta_-^2}}{\sqrt{(\kappa^2 - \gamma^2)^2 + \gamma^2 \Delta_-^2}}. \quad (\text{E2})$$

Since  $\Delta_- = |\Delta_2 - \Delta_1| \ll \kappa, \gamma$ , the effective optomechanical coupling strength  $g_{\text{eff}}$  can be greatly amplified in the vicinity of EP when  $\kappa \rightarrow \gamma$ . This means that in this case the effective optomechanical coupling strength  $g_{\text{eff}}$  can be greatly enhanced. Given the parameters, we can obtain the simulation results of the effective optomechanical coupling strength  $g_{\text{eff}}$  versus the optical coupling strength  $\kappa$ , as shown in Fig. 10. When the optical coupling strength  $\kappa$  is far away from the exceptional point, i.e., in the green area in Fig. 10, the effective optomechanical coupling strength changes linearly with the optical coupling strength  $\kappa$ . However, in the pink area,  $g_{\text{eff}}$  increases very fast when the system approaches to EP, which means that in this regime the optomechanical interaction can be greatly amplified. In addition, by comparing Eq. (E2) with Eq. (C1) and Eq. (C2),

we can find that  $|\delta\Omega_{1,2}| \propto g_{\text{eff}}^4 |f_1(\kappa, \gamma, \epsilon, g_{\text{om}}, \Delta_-)|$ , and  $\kappa_{\text{mech}} \propto g_{\text{eff}}^4 |f_2(\kappa, \gamma, \epsilon, g_{\text{om}}, \Delta_-)|$ , which means that the enhanced optomechanical coupling strength can lead to improvements of the optomechanics-induced mechanical frequency shifts and the effective mechanical coupling in the vicinity of EP.

#### Appendix F: The difference between active $\mathcal{PT}$ -symmetric system and passive system with EP for synchronization

Based on the previous discussion, we know that in the discussed gain-loss balanced  $\mathcal{PT}$ -symmetric optomechanical system, there exists amplifications of the optomechanics-induced mechanical frequency shifts and effective mechanical coupling strength in the vicinity of exceptional point. However, if this  $\mathcal{PT}$ -symmetric system is replaced by a passive coupled system with an exceptional point, i.e., the active resonator in the discussed  $\mathcal{PT}$ -symmetric system is replaced by a passive resonator, the two far-detuned mechanical modes in this system cannot synchronize with each other. To show this, we can easily obtain the dynamical equations of the system by replacing the optical damping  $\gamma_1$  in Eq. (1) with  $-\gamma_1$

$$\begin{aligned} \dot{\alpha}_1 &= (-\gamma_1 - i\Delta_1)\alpha_1 - i\kappa\alpha_2 - ig_{\text{om}}\alpha_1(\beta_1 + \beta_1^*) \\ &\quad + \sqrt{2\gamma_{1\text{ex}}}\epsilon_1, \\ \dot{\alpha}_2 &= (-\gamma_2 - i\Delta_2)\alpha_2 - i\kappa\alpha_1 - ig_{\text{om}}\alpha_2(\beta_2 + \beta_2^*) \\ &\quad + \sqrt{2\gamma_{2\text{ex}}}\epsilon_2, \\ \dot{\beta}_1 &= -(\Gamma_{m1} + i\Omega_1)\beta_1 - ig_{\text{om}}|\alpha_1|^2, \\ \dot{\beta}_2 &= -(\Gamma_{m2} + i\Omega_2)\beta_2 - ig_{\text{om}}|\alpha_2|^2. \end{aligned} \quad (\text{F1})$$

Under the assumptions that  $\sqrt{2\gamma_{1\text{ex}}}\epsilon_1 = \sqrt{2\gamma_{2\text{ex}}}\epsilon_2 = \epsilon$ , and  $\Delta_{1,2}, |\Delta_2 - \Delta_1| \ll \kappa, \gamma_{1,2}$ , the optomechanics-induced mechanical frequency shifts  $\delta\Omega_{1,2}$  and the effective mechanical coupling  $\kappa_{\text{mech}}$  can be approximately expressed as

$$\begin{aligned} \delta\Omega_1 &= -\delta\Omega_2 \approx g_{\text{om}}^2 \frac{\Delta_- \epsilon^2}{[(\kappa^2 + \gamma_1 \gamma_2) + \Delta_+^2]^2}, \\ \kappa_{\text{mech}} &\approx 2g_{\text{om}}^2 \frac{\kappa \epsilon^2}{[(\kappa^2 + \gamma_1 \gamma_2) + \Delta_+^2]^2}, \end{aligned} \quad (\text{F2})$$

where  $\Delta_+ = (\Delta_1 + \Delta_2)/2$  and  $\Delta_- = \Delta_2 - \Delta_1$ . As  $\Delta_- \ll \kappa, \gamma_{1,2}$  and  $g_{\text{om}}$  is very tiny,  $\delta\Omega_{1,2}$  and  $\kappa_{\text{mech}}$  are very small. This implies that in this passive system with an exceptional point, the amplifications of mechanical frequency shifts and effective mechanical coupling are not strong enough. Thus these two mechanical modes with far-off-resonant mechanical frequencies cannot be synchronized.

In addition, if the balance between gain and loss is broken in our  $\mathcal{PT}$ -symmetric system, i.e.,  $\Gamma_- = |\gamma_1 - \gamma_2|/2 \neq 0$ , the synchronization between the two mechanical modes will be suppressed. In fact, when the bal-

ance between gain and loss is broken, the mechanical frequency shifts  $\delta\Omega_{1,2}$  and the effective mechanical coupling  $\kappa_{\text{mech}}$  can be expressed as

$$\begin{aligned}\delta\Omega_1 &\approx 2g_{om}^2 \frac{\Delta_-(\kappa^2 + \gamma_2^2)^2\epsilon^2}{\left[(\kappa^2 - \gamma_1\gamma_2)^2 + (\gamma_1 + \gamma_2)^2\Delta_-^2/4 + \Gamma_-^2\Delta_+^2\right]^2}, \\ \delta\Omega_2 &\approx 2g_{om}^2 \frac{\Delta_-(\kappa^2 + \gamma_1^2)^2\epsilon^2}{\left[(\kappa^2 - \gamma_1\gamma_2)^2 + (\gamma_1 + \gamma_2)^2\Delta_-^2/4 + \Gamma_-^2\Delta_+^2\right]^2}, \\ \kappa_{\text{mech}} &\approx 4g_{om}^2 \frac{\Delta_-\kappa^2\gamma_1\gamma_2\epsilon^2}{\left[(\kappa^2 - \gamma_1\gamma_2)^2 + (\gamma_1 + \gamma_2)^2\Delta_-^2/4 + \Gamma_-^2\Delta_+^2\right]^2}.\end{aligned}\quad (\text{F3})$$

Therefore, with the increase of  $\Gamma_-$ , the amplification effects of the mechanical frequency shifts and the effective mechanical coupling strength will be suppressed. We show the mechanical frequency shifts  $\delta\Omega_{1,2}$  and the effective mechanical coupling strength  $\kappa_{\text{mech}}$  with different  $\Gamma_-$  in Figs. 11 (a), (b), and (c), respectively. It can be clearly seen that the amplifications of the mechanical frequency shifts and the effective mechanical coupling strength are seriously suppressed when  $\Gamma_-$  is large, thus the synchronization between the two mechanical modes with far-off-resonant cannot be realized.

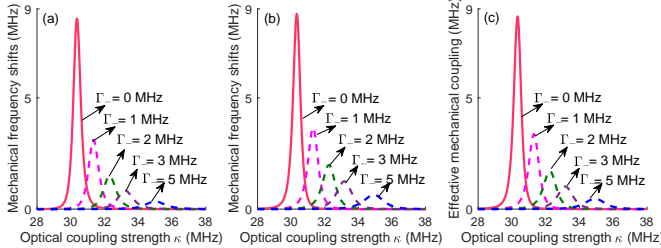


FIG. 11: (Color online) (a) Optomechanics-induced mechanical frequency shifts  $\delta\Omega_1$  versus the optical coupling strength  $\kappa$  with different  $\Gamma_-$ . The solid curve denotes the case that gain and loss are balanced, i.e.,  $\Gamma_- = 0$ . It is shown that the amplification effects of  $\delta\Omega_1$  are suppressed with the increase of  $\Gamma_-$ . (b) Corresponding to the optomechanics-induced mechanical frequency shifts  $-\delta\Omega_2$  versus the optical coupling strength  $\kappa$  with different  $\Gamma_-$ . (c) Effective mechanical coupling  $\kappa_{\text{mech}}$  between the two mechanical modes versus the optical coupling strength  $\kappa$  with different  $\Gamma_-$ . It is shown that the amplification effects of  $\kappa_{\text{mech}}$  are also suppressed with the increase of  $\Gamma_-$ .

## Appendix G: Derivation of the normalized correlation function $R$

To simplify our discussions, we redefine four variables

$$\begin{aligned}\xi_1 &= x_1, & \xi_2 &= \dot{x}_1, \\ \xi_3 &= x_2, & \xi_4 &= \dot{x}_3,\end{aligned}\tag{G1}$$

thus the Langevin equation of the mechanical modes (Eq. 7) can be re-expressed as

$$\begin{aligned} \begin{bmatrix} \dot{\xi}_1(t) \\ \dot{\xi}_2(t) \\ \dot{\xi}_3(t) \\ \dot{\xi}_4(t) \end{bmatrix} &= - \begin{bmatrix} 0 & -1 & 0 & 0 \\ \tilde{\Omega}_1^2 & 2\Gamma_m & \kappa_{\text{mech}} & 0 \\ 0 & 0 & 0 & -1 \\ \kappa_{\text{mech}} & 0 & \tilde{\Omega}_2^2 & 2\Gamma_m \end{bmatrix} \begin{bmatrix} \xi_1(t) \\ \xi_2(t) \\ \xi_3(t) \\ \xi_4(t) \end{bmatrix} + \begin{bmatrix} \Gamma_1 \\ \Gamma_2 \\ \Gamma_3 \\ \Gamma_4 \end{bmatrix} \\ &= -A \begin{bmatrix} \xi_1(t) \\ \xi_2(t) \\ \xi_3(t) \\ \xi_4(t) \end{bmatrix} + \begin{bmatrix} \Gamma_1 \\ \Gamma_2 \\ \Gamma_3 \\ \Gamma_4 \end{bmatrix}, \end{aligned} \quad (\text{G2})$$

where  $\Gamma_1 = \Gamma_3 = 0$ ;  $\Gamma_2 = \Gamma_{\text{noise1}}$ ; and  $\Gamma_4 = \Gamma_{\text{noise2}}$ . The solution of the above equation can be expressed as

$$\xi_i(t) = \sum_{k=1}^4 G_{ik}(t) z_k + \sum_{k=1}^4 \int_0^t G_{ik}(t') \Gamma_k(t-t') dt', \quad (G3)$$

where matrix  $G = (G_{ij}) = \exp(-At)$ , and  $z_i$  represent the initial values of the variables  $\xi_i$ . As we consider small time  $t$ , the matrix  $G$  can be approximately expressed as

$$\begin{aligned}
G(t) &= e^{-At} \\
&\approx I - At \\
&\approx \begin{bmatrix} 1 & t & 0 & 0 \\ -\tilde{\Omega}_1^2 t & 1 - 2\Gamma_m t & -\kappa_{\text{mech}} t & 0 \\ 0 & 0 & 1 & t \\ -\kappa_{\text{mech}} t & 0 & -\tilde{\Omega}_2^2 t & 1 - 2\Gamma_m t \end{bmatrix}, \tag{G4}
\end{aligned}$$

thus the solution of  $\xi_1(t)$  in Eq. (G3) can be approximately expressed as

$$\begin{aligned}
 \xi_1(t) &= G_{11}z_1 + G_{12}z_2 + G_{13}z_3 + G_{14}z_4 \\
 &\quad + \int_0^t G_{11}(t')\Gamma_1(t-t') + G_{12}(t')\Gamma_2(t-t') \\
 &\quad + G_{13}(t')\Gamma_3(t-t') + G_{14}(t')\Gamma_4(t-t')dt' \\
 &= z_1 + tz_2 + \int_0^t t'\Gamma_2(t-t')dt'. \tag{G5}
 \end{aligned}$$

Similarly, other solutions in Eq. (G3) can be approximately expressed as

$$\begin{aligned}
\xi_2(t) &= - \left( \kappa_{\text{mech}} z_3 + \tilde{\Omega}_1^2 z_1 \right) t + (1 - 2\Gamma_m t) z_2 \\
&\quad + \int_0^t (1 - 2\Gamma_m t') \Gamma_2(t - t') dt', \\
\xi_3(t) &= z_3 + z_4 t + \int_0^t t' \Gamma_4(t - t') dt', \\
\xi_4(t) &= - \left( \kappa_{\text{mech}} z_1 + \tilde{\Omega}_2^2 z_3 \right) t + (1 - 2\Gamma_m t) z_4 \\
&\quad + \int_0^t (1 - 2\Gamma_m t') \Gamma_4(t - t') dt'. \tag{G6}
\end{aligned}$$

We then calculate the correlation functions as

$$R_{ij}(\tau, t) = \langle \xi_i(t + \tau) \xi_j(t) \rangle, \quad (G7)$$

where  $\langle \cdot \rangle$  is the ensemble average over the stochastic noises. Based on the regression theorem [68], we know that the correlation functions  $R_{ij}(\tau, t)$  can be reduced to

$$R_{ij}(\tau, t) = \sum_{k=1}^4 G_{ik}(\tau) \langle \xi_k(t) \xi_j(t) \rangle, \quad 0 \leq \tau. \quad (\text{G8})$$

By substituting the solutions of  $\xi_i(t)$  as shown in Eqs. (G5) and (G6) into the correlation functions  $R_{ij}(\tau, t)$  (Eq. (G8)), the three correlation functions  $R_{13}(\tau, t)$ ,  $R_{11}(0, t)$ , and  $R_{33}(0, t)$  can be expressed as

$$\begin{aligned} R_{13}(\tau, t) &= (z_1 + tz_2)(z_3 + z_4t) + \frac{q}{3}t^3 \\ &+ \tau \left[ -\left( \kappa_{\text{mech}}z_3 + \tilde{\Omega}_1^2 z_1 \right) (z_3 + z_4t)t \right. \\ &\left. + (1 - 2\Gamma_m t)(z_3 + z_4t)z_2 + q \left( \frac{1}{2}t^2 - \frac{2}{3}\Gamma_m t^3 \right) \right], \\ R_{11}(0, t) &= (z_1 + z_2t)^2 + \frac{q}{3}t^3, \\ R_{33}(0, t) &= (z_3 + z_4t)^2 + \frac{q}{3}t^3. \end{aligned} \quad (\text{G9})$$

For simplicity we assume that the system is stationary at the initial time, i.e.,  $z_2 = z_4 = 0$ , and consider the case that  $z_1 = 1/\tilde{\Omega}_1^2$ ,  $z_3 = 1/\kappa_{\text{mech}}$ , thus the normalized correlation function between the two mechanical modes can be expressed as

$$\begin{aligned} R(\tau, t) &= \frac{|R_{13}(\tau, t)|}{\sqrt{R_{11}(0, t)} \sqrt{R_{33}(0, t)}} \\ &= \frac{\left| 1 - 2\tilde{\Omega}_1^2 \tau t + q \frac{\kappa_{\text{mech}} \tilde{\Omega}_1^2}{2} \tau t^2 + q \frac{\kappa_{\text{mech}} \tilde{\Omega}_1^2}{3} \tau t^3 \right|}{\sqrt{1 + \frac{q}{3} \kappa_{\text{mech}}^2 t^3} \sqrt{1 + \frac{q}{3} \tilde{\Omega}_1^4 t^3}} \\ &\approx 1 - 2\tilde{\Omega}_1^2 \tau t + \frac{q}{2} \kappa_{\text{mech}} \tilde{\Omega}_1^2 \tau t^2 + \frac{q}{3} \kappa_{\text{mech}} \tilde{\Omega}_1^2 \tau t^3 \\ &\approx 1 - 2\tilde{\Omega}_1^2 \tau t + 2\Gamma_m k T \kappa_{\text{mech}} \tilde{\Omega}_1^2 \tau t^2 \\ &\quad + \frac{4}{3} \Gamma_m k T \kappa_{\text{mech}} \tilde{\Omega}_1^2 \tau t^3. \end{aligned} \quad (\text{G10})$$

---

[1] A. S. Pikovsky, M. Rosenblum, and J. Kurths, *Synchronization—A Unified Approach to Nonlinear Science* (Cambridge University Press, Cambridge, UK, 2001).

[2] R. Brown and L. Kocarev, A Unifying Definition of Synchronization for Dynamical Systems, *Chaos*, **10**, 344 (2000).

[3] L. Glass, M. C. Mackey, *From Clocks to Chaos: The Rhythms of Life* (Princeton Univ. Press, Princeton, NJ, 1988).

[4] A. T. Winfree, *The Geometry of Biological Time* (Springer, New York, ed. 2, 2001).

[5] A. Goldbeter, *Biochemical Oscillations and Cellular Rhythms: The Molecular Bases of Periodic and Chaotic Behaviour* (Cambridge Univ. Press, Cambridge, 1996).

[6] A. F. Taylor, M. R. Tinsley, F. Wang, Z. Y. Huang, and K. Showalter, Dynamical quorum sensing and synchronization in large populations of chemical oscillators, *Science* **323**, 614 (2009).

[7] S. H. Strogatz, *Sync: The Emerging Science of Spontaneous Order* (Hyperion, New York, 2003), 1st ed.

[8] S. C. Manrubia, A. S. Mikhailov, D. H. Zanette, *Emergence of Dynamical Order: Synchronization Phenomena in Complex Systems* (World Scientific, Singapore, 2004).

[9] S. Bregni, *Synchronization of Digital Telecommunications Networks* (Wiley, Chichester, 2002).

[10] M. Aspelmeyer, T. J. Kippenberg, and F. Marquardt, Cavity optomechanics, *Rev. Mod. Phys.* **86**, 1391 (2014).

[11] C. A. Holmes, C. P. Meaney, and G. J. Milburn, Synchronization of many nanomechanical resonators coupled via a common cavity field, *Phys. Rev. E* **85**, 066203 (2012).

[12] T. Li, T. Y. Bao, Y. L. Zhang, C. L. Zou, X. B. Zou, and G. C. Guo, Long-distance synchronization of unidirectionally cascaded optomechanical systems, *Opt. Exp.* **24**, 12338 (2016).

[13] M. Zhang, G. S. Wiederhecker, S. Manipatruni, A. Barnard, P. McEuen, and M. Lipson, Synchronization of micromechanical oscillators using light, *Phys. Rev. Lett.* **109**, 233906 (2012).

[14] M. Bagheri, M. Poot, L. Fan, F. Marquardt, and H. X. Tang, Photonic cavity synchronization of nanomechanical oscillators, *Phys. Rev. Lett.* **111**, 213902 (2013).

[15] S. Y. Shah, M. Zhang, R. Rand, and M. Lipson, Master-slave locking of optomechanical oscillators over a long distance, *Phys. Rev. Lett.* **114**, 113602 (2015).

[16] N. Yang, A. Miranowicz, Y. C. Liu, K. Xia, and F. Nori, Chaotic synchronization of two optical modes in optomechanical systems, *Sci. Rep.* **9**, 15874 (2019).

[17] H. Xu, D. Mason, L. Jiang, and G. E. Harris, Topological energy transfer in an optomechanical system with exceptional points, *Nature* **537**, 80 (2016).

[18] H. Jing, S. K. Özdemir, X. Y. Lü, J. Zhang, L. Yang, and F. Nori, PT-Symmetric phonon laser, *Phys. Rev. Lett.* **113**, 053604 (2014).

[19] D. W. Schönleber, A. Eisfeld, and R. El-Ganainy, Optomechanical interactions in non-Hermitian photonic molecules, *New J. Phys.* **18**, 045014 (2016).

[20] Z. P. Liu, J. Zhang, S. K. Özdemir, B. Peng, H. Jing, X. Y. Lü, C. W. Li, L. Yang, F. Nori, and Y. X. Liu, Metrology with PT-symmetric cavities: enhanced sensitivity near the PT-phase transition, *Phys. Rev. Lett.* **117**, 110802 (2016).

[21] H. Jing, S. K. Özdemir, Z. Geng, J. Zhang, X. Y. Lü, B. Peng, L. Yang, and F. Nori, Optomechanically-induced transparency in parity-time-symmetric microresonators, *Sci. Rep.* **5**, 9663 (2015).

[22] X. Y. Lü, H. Jing, J. Y. Ma, and Y. Wu, PT-symmetry-breaking Chaos in Optomechanics, *Phys. Rev. Lett.* **114**,

253601 (2015).

[23] J. Zhang, P. Bo, S. K. Özdemir, Y. X. H. Jing, X. Y. Lü, Y. L. Liu, L. Yang, and F. Nori, Giant nonlinearity via breaking parity-time symmetry: a route to low-threshold phonon diodes, *Phys. Rev. B* **92**, 115407 (2015).

[24] C. M. Bender and S. Boettcher, Real spectra in non-Hermitian Hamiltonians having PT symmetry, *Phys. Rev. Lett.* **80**, 5243 (1998).

[25] C. M. Bender, Making sense of non-Hermitian Hamiltonians, *Rep. Prog. Phys.* **70**, 947 (2007).

[26] G. S. Agarwal and K. Qu, Spontaneous generation of photons in transmission of quantum fields in  $\mathcal{PT}$ -symmetric optical systems, *Phys. Rev. A* **85**, 031802 (2012).

[27] A. Mostafazadeh, Pseudo-Hermiticity versus PT symmetry: the necessary condition for the reality of the spectrum of a non-Hermitian Hamiltonian, *J. Math. Phys.* **43**, 205 (2002).

[28] B. Peng, S. K. Özdemir, F. C. Lei, F. Monifi, M. Giannfreda, G. L. Long, S. H. Fan, F. Nori, C. M. Bender, and L. Yang, Parity-time-symmetric whispering-gallery microcavities, *Nat. Phys.* **10**, 394 (2014).

[29] L. Feng, Z. J. Wong, R. M. Ma, Y. Wang, and X. Zhang, Singlemode laser by parity-time symmetry breaking, *Science* **346**, 972 (2014).

[30] H. Hodaei, M. A. Miri, M. Heinrich, D. N. Christodoulides, and M. Khajavikhan, Parity-time-symmetric microring lasers, *Science* **346**, 975 (2014).

[31] A. Guo, G. J. Salamo, D. Duchesne, R. Morandotti, M. Volatier-Ravat, V. Aimez, G. A. Siviloglou, and D. N. Christodoulides, Observation of PT-symmetry breaking in complex optical potentials, *Phys. Rev. Lett.* **103**, 093902 (2009).

[32] C. E. Rüter, K. G. Makris, R. El-Ganainy, D. N. Christodoulides, M. Segev, and D. Kip, Observation of parity-time symmetry in optics, *Nat. Phys.* **6**, 192 (2010).

[33] H. Ramezani, T. Kottos, R. El-Ganainy, and D. N. Christodoulides, Unidirectional nonlinear PT-symmetric optical structures, *Phys. Rev. A* **82**, 043803 (2010).

[34] Z. Lin, H. Ramezani, T. Eichelkraut, T. Kottos, H. Cao, and D. N. Christodoulides, Unidirectional invisibility induced by PT-symmetric periodic structures, *Phys. Rev. Lett.* **106**, 213901 (2011).

[35] L. Feng, M. Ayache, J. Huang, Y. L. Xu, M. H. Lu, Y. F. Chen, Y. Fainman, and A. Scherer, Nonreciprocal light propagation in a silicon photonic circuit, *Science* **333**, 729 (2011).

[36] A. Regensburger, C. Bersch, M. A. Miri, G. Onishchukov, D. N. Christodoulides, and U. Peschel, Parity-time synthetic photonic lattices, *Nature (London)* **488**, 167 (2012).

[37] L. Chang, X. S. Jiang, S. Y. Hua, C. Yang, J. M. Wen, L. Jiang, G. Y. Li, G. Z. Wang, and M. Xiao, Parity-time symmetry and variable optical isolation in active-passive-coupled microresonators, *Nat. Photonics.* **8**, 524 (2014).

[38] B. Peng, S. K. Özdemir, S. Rotter, H. Yilmaz, M. Liertzer, F. Monifi, C. M. Bender, F. Nori, and L. Yang, Loss induced suppression and revival of lasing, *Science* **346**, 328 (2014).

[39] J. Schindler, A. Li, M. C. Zheng, F. M. Ellis, and T. Kottos, Experimental study of active LRC circuits with PT symmetries. *Phys. Rev. A* **84**, 040101(R) (2011).

[40] C. T. West, T. Kottos, and T. Prosen, PT-symmetric wave chaos. *Phys. Rev. Lett.* **104**, 054102 (2015).

[41] J. Wiersig, Enhancing the sensitivity of frequency and energy splitting detection by using exceptional points: application to microcavity sensors for single-particle detection. *Phys. Rev. Lett.* **112**, 203901 (2014).

[42] W. Chen, S. K. Ozdemir, G. Zhao, J. Wiersig, and L. Yang, Exceptional points enhance sensing in an optical microcavity, *Nature* **548**, 192-196 (2017).

[43] H. Hodaei, A. U. Hassan, S. Wittek, H. Garcia-Gracia, R. El-Ganainy, D. N. Christodoulides, and M. Khajavikhan, Enhanced sensitivity at higher-order exceptional points, *Nature* **548**, 187-191 (2017).

[44] J. Doppler, A. A. Mailybaev, J. Bohm, U. Kuhl, A. Girschik, F. Libisch, T. J. Milburn, P. Rabl, N. Moiseyev, and S. Rotter, Dynamically encircling an exceptional point for asymmetric mode switching, *Nature* **537**, 76-79 (2016).

[45] X. Zhou and Y. D. Chong,  $\mathcal{PT}$  symmetry breaking and nonlinear optical isolation in coupled microcavities, *Opt. Express* **24**, 6916 (2016).

[46] A. U. Hassan, H. Hodaei, M. A. Miri, M. Khajavikhan, and D. N. Christodoulides, *Phys. Rev. A* **92**, 063807 (2015).

[47] R. N. Bracewell, *The Fourier Transform and Its Applications* (McGraw-Hill, New York, 1978).

[48] L. R. Rabiner and R. W. Schafer, *Digital Processing of Speech Signals* (Prentice-Hall, Englewood Cliffs, NJ, 1978).

[49] N. A. Anstey, Correlation Techniques—A Review, *Can. J. Expl. Geophys.*, **2**, 55 (1966).

[50] P. H. White, Cross Correlation in Structural Systems: Dispersion and Nondispersion Waves, *J. Acoust. Soc. Am.* **45**, 1118 (1969).

[51] M. V. Heel, Similarity measures between images, *Ultrasound* **21**, 95 (1987).

[52] J. P. Lewis, Fast Normalized Cross-Correlation, *Proc. Vision Interface*, 120 (1995). J. C. Yoo and T. H. Han, Fast Normalized Cross-Correlation, *Circuits Syst Signal Process* **28**, 819 (2009).

[53] A. Neiman, Synchronizationlike phenomena in coupled stochastic bistable systems, *Phys. Rev. E* **49**, 3484 (1994).

[54] S. K. Han, T. G. Yim, D. E. Postnov and O. V. Sosnovtseva, Interacting coherence resonance oscillators, *Phys. Rev. Lett.* **83**, 1771 (1999).

[55] A. Neiman, L. Schimansky-Geier, A. Cornell-Bell, and F. Moss, Noise-enhanced phase synchronization in excitable media, *Phys. Rev. Lett.* **83**, 4896 (1999).

[56] H. Nakao, K. Arai, and Y. Kawamura, Noise-induced synchronization and clustering in ensembles of uncoupled limit-cycle oscillators, *Phys. Rev. Lett.* **98**, 184101 (2007).

[57] K. H. Nagai and H. Kori, Noise-induced synchronization of a large population of globally coupled nonidentical oscillators, *Phys. Rev. E* **81**, 065202 (2010).

[58] Y. M. Lai and M. A. Porter, Noise-induced synchronization, desynchronization, and clustering in globally coupled nonidentical oscillators, *Phys. Rev. E* **88**, 012905 (2013).

[59] C. S. Zhou and J. Kurths, Noise-induced Phase synchronization and synchronization transitions in chaotic oscillators, *Phys. Rev. Lett.* **88**, 230602 (2002).

[60] D. H. He, P. L. Shi, and L. Stone, Noise-induced synchronization in realistic models, *Phys. Rev. E* **67**, 027201

(2003).

[61] H. Schomerus, Quantum noise and self-sustained radiation of PT-symmetric systems, *Phys. Rev. Lett.* **104**, 233601 (2010).

[62] S.-Y. Lee, J.-W. Ryu, J.-B. Shim, S.-B. Lee, S. W. Kim, and K. An, Divergent Petermann factor of interacting resonances in a stadium-shaped microcavity, *Phys. Rev. A* **78**, 015805 (2008).

[63] G. Yoo, H.-S. Sim, and H. Schomerus, Quantum noise and mode nonorthogonality in non-Hermitian PT-symmetric optical resonators, *Phys. Rev. A* **84**, 063833 (2011).

[64] J. Zhang, B. Peng, S. K. Ozdemir, S. Rotter, K. Pichler, D. Krimer, G. Zhao, F. Nori, Y.-X. Liu, and L. Yang, A phonon laser operating at the exceptional point, *Nat. Photonics* **12**, 479 (2018).

[65] H. A. Kramers, Brownian motion in a field of force and the diffusion model of chemical reactions, *Physica* **7**, 284 (1940).

[66] G. Klein, Mean first-passage times of Brownian motion and related problems, *R. Soc. London A* **211**, 431 (1952).

[67] H. Hofmann and F. A. Ivanyuk, Mean first passage time for nuclear fission and the emission of light particles, *Phys. Rev. Lett.* **90**, 132701 (2003).

[68] H. Risken, *The Fokker-Planck Equation: Methods of Solution and Applications*, 2nd ed. (Springer, Berlin, 1989).